

AD-A040 388

MASSACHUSETTS INST OF TECH CAMBRIDGE
FIBER/MATRIX INTERACTION EFFECTS ON FRACTURE TOUGHNESS OF STRUC--ETC(U)
JUL 75 D G PIRES, J F MANDELL, C E FONG

F/G 11/4

DAAG46-72-C-0233

AMMRC-CTR-75-15

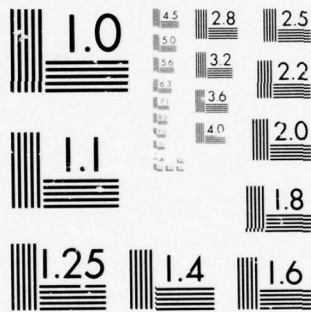
NL

UNCLASSIFIED

1 OF 2

AD
A040388





AD A 040388



AD

11

AMMRC CTR 75-15

FIBER/MATRIX INTERACTION EFFECTS
ON STRUCTURE TOUGHNESS
OF STRUCTURAL COMPOSITES

July 1975

D.G. Pires,
C.E. Fong,
J.F. Mandell,
F.J. McGarry

Massachusetts Institute of Technology
Cambridge, Massachusetts 03139

DDC
RECEIVED
JUN 10 1977
A

FINAL REPORT

CONTRACT NUMBER DAAG-46-72-C-0233

Approved for public release; distribution unlimited.

Prepared for

ARMY MATERIALS AND MECHANICS RESEARCH CENTER
Watertown, Massachusetts 02172

AD No. _____
DDC FILE COPY

The findings in this report are not to be construed as an official Department of the Army position, unless so designated by other authorized documents.

Mention of any trade names or manufacturers in this report shall not be construed as advertising nor as an official indorsement or approval of such products or companies by the United States Government.

DISPOSITION INSTRUCTIONS

Destroy this report when it is no longer needed.
Do not return it to the originator.

UNCLASSIFIED

SECURITY CLASSIFICATION OF THIS PAGE (When Data Entered)

| 19 REPORT DOCUMENTATION PAGE | | READ INSTRUCTIONS BEFORE COMPLETING FORM | |
|---|-----------------------|---|--|
| 1. REPORT NUMBER | 2. GOVT ACCESSION NO. | 3. RECIPIENT'S CATALOG NUMBER | |
| 18 AMMRC CTR-75-15 ✓ | | | |
| 4. TITLE (and Subtitle) | | 5. TYPE OF REPORT & PERIOD COVERED | |
| 6 FIBER/MATRIX INTERACTION EFFECTS ON FRACTURE TOUGHNESS OF STRUCTURAL COMPOSITES. | | 9 Final Report, JULY 1975 | |
| 7. AUTHOR(s) | | 8. CONTRACT OR GRANT NUMBER(s) | |
| 10 D.G./PIRES, C.E./FONG, J.F./MANDELL, and F.J./McGARRY | | 15 DAAG 46-72-c-0233 ✓ | |
| 9. PERFORMING ORGANIZATION NAME AND ADDRESS | | 10. PROGRAM ELEMENT, PROJECT, TASK AREA & WORK UNIT NUMBERS | |
| Massachusetts Institute of Technology 77 Massachusetts Avenue, Cambridge, Mass. 02139 | | D/A Project: AMCMS Code: Agency Accession: | |
| 11. CONTROLLING OFFICE NAME AND ADDRESS | | 12. REPORT DATE | |
| Army Materials and Mechanics Research Center Watertown, Massachusetts 02172 | | 11 July 1975 ✓ | |
| 14. MONITORING AGENCY NAME & ADDRESS (if different from Controlling Office) | | 13. NUMBER OF PAGES | |
| 12 106p. | | 103 | |
| | | 15. SECURITY CLASS. (of this report) | |
| | | Unclassified | |
| | | 15a. DECLASSIFICATION/DOWNGRADING SCHEDULE | |
| 16. DISTRIBUTION STATEMENT (of this Report) | | | |
| Approved for public release; distribution unlimited. | | | |
| 17. DISTRIBUTION STATEMENT (of the abstract entered in Block 20, if different from Report) | | | |
| 18. SUPPLEMENTARY NOTES | | | |
| 19. KEY WORDS (Continue on reverse side if necessary and identify by block number) | | | |
| Composite Materials Surface finishing Toughness Woven fiber Composites Fiber reinforced Plastics Crack Propagation Fiber matrix bonding Fracture (materials) | | | |
| 20. ABSTRACT (Continue on reverse side if necessary and identify by block number) | | | |
| <p>→ The object of the study was to relate the effects of fiber, matrix and interface to the fracture toughness of fiber reinforced plastic composites. The initial part of the study employed a model composite system to determine</p> <p style="text-align: right;">→ over</p> | | | |

UNCLASSIFIED

SECURITY CLASSIFICATION OF THIS PAGE(When Data Entered)

the resistance to crack propagation normal to the fibers. Laminates suitable for projectile impact tests were also used to determine the resistance to interlaminar crack propagation between plies. Subsequently, a series of projectile impact tests were conducted on the laminates at AMMRC. After some delay, another series of fracture tests were conducted at M.I.T. on the systems which showed extremes in projectile impact resistance. This last series of tests was designed to determine the resistance to crack propagation normal to the fibers for laminates representative of those used in the projectile impact tests, as distinct from the earlier tests on model systems.

The results of the program indicate that fiber and matrix properties bear a clear relationship to the model composite toughness, while the effects of changes in the interface also are important in some cases. Correlations between the fracture toughness and projectile impact resistance are tenuous in most cases.

UNCLASSIFIED

SECURITY CLASSIFICATION OF THIS PAGE(When Data Entered)

FIBER/MATRIX INTERACTION EFFECTS
ON FRACTURE TOUGHNESS OF
STRUCTURAL COMPOSITES

JULY 1975

D. G. PIRES, C. E. FONG,
J. F. MANDELL, and F. J. McGARRY
Massachusetts Institute of Technology

Final Report - Contract Number DAAG46-72-C-0233

Prepared for
ARMY MATERIALS AND MECHANICS RESEARCH CENTER
Watertown, Massachusetts 02172

| | |
|---------------------------------|--|
| ACCESSION NO. | |
| NTIS | SPRINT CATALOG <input checked="" type="checkbox"/> |
| DDC | DDC CATALOG <input type="checkbox"/> |
| UNANNOUNCED | <input type="checkbox"/> |
| JUSTIFICATION | |
| BY | |
| DISTRIBUTION AVAILABILITY CODES | |
| Dist. | STANDARD SPECIAL |
| A | |

ABSTRACT

The object of the study was to relate the effects of fiber, matrix, and interface to the fracture toughness of fiber reinforced plastic composites. The initial part of the study employed a model composite system to determine the resistance to crack propagation normal to the fibers. Laminates suitable for projectile impact tests were also used to determine the resistance to interlaminar crack propagation between plies. Subsequently, a series of projectile impact tests were conducted on the laminates at AMMRC. After some delay, another series of fracture tests were conducted at M.I.T. on the systems which showed extremes in projectile impact resistance. This last series of tests was designed to determine the resistance to crack propagation normal to the fibers for laminates representative of those used in the projectile impact tests, as distinct from the earlier tests on model systems.

The results of the program indicate that fiber and matrix properties bear a clear relationship to the model composite toughness, while the effects of changes in the interface also are important in some cases. Correlations between the fracture toughness and projectile impact resistance are tenuous in most cases.

I. Introduction

The purpose of the work described in this report was to investigate the effects of fiber/matrix interactions on the toughness of fiber reinforced plastics. The study was split into two parts: the first investigated the toughness and debonding characteristics of five fibers, two matrices, and two fiber surface treatments on the interlaminar toughness and on the toughness of model composites where the crack propagated normal to the fibers; the second investigated the toughness of four selected fiber/matrix/interface conditions for cracks propagating in the warp direction of laminates containing realistic fiber volume fractions. Separate reports were prepared for each part of the work and these give complete details as to background material, experimental techniques, results, discussion, and conclusions. Appendix A gives the report prepared from the first portion of the study; Appendix B gives results for Kevlar fibers which were not included in Appendix A, but were completed during the extension period; and Appendix C gives the report on the main effort of the extended time period. While all details of the complete study are given in Appendices A, B, and C, the initial sections of the report will provide a summary of the findings and a discussion of the overall implications as they relate to the anticipated usefulness of the fracture toughness as an index of projectile impact performance.

MATERIALS AND EXPERIMENTAL TECHNIQUES

The first part of the study (Appendix A) involved determination of the fracture toughness for various fiber/matrix/interface combinations. The fibers investigated were E-glass, S-glass, Low Modulus (LM) glass, and PRD 49-III and IV (Kevlar 49 and 29); the matrices were polyester (Paraplex P-43, Rohm and Haas, Inc.) and vinylester (Derakane 411-45, Dow Chemical Co.,) the fiber surfaces were acetone-cleaned as received for good adhesion, and starch-oil sized for poor adhesion. The toughness for a crack propagating normal to the fibers was measured with a model double-cantilever beam specimen. The model was constructed by locating individual yarns of fibers in the path of the crack; the low fiber volume fraction, usually less than one percent, discouraged crack deflection to a direction parallel to the fibers as commonly occurs at higher fiber volume fractions. The toughness (fracture surface work) and debonding length along the yarn were determined for each system. In addition to the model system, a second fracture test was conducted on laminates of high fiber volume fraction (approximately 65%) by propagating a crack between the plies using a similar cleavage-type test specimen. Thus, the toughness for crack propagation both normal to the fibers and between the plies was investigated. In a subsequent study at AMMRC, projectile impact tests also were run on a number of the laminates fabricated in this phase.

The second part of the study (Appendix C) was concerned with crack propagation normal to the fibers in laminates of high fiber volume fraction. Only those cases which proved to have the best and worst projectile impact performances were explored: S-glass woven roving, acetone cleaned, with polyester and vinylester matrices were the two worst cases; E-glass and S-glass woven roving, starch-oil finish, polyester matrix were the two best cases. It should be noted that only those systems with woven roving reinforcement were projectile impact tested, eliminating the Kevlar laminates from consideration. The four systems were fabricated into laminates and tested using a standard notched-tension specimen to measure the critical stress-intensity factor and the notch sensitivity.

RESULTS

Detailed results are presented for each case in the appendices, and only a summary of the more prominent findings will be given here.

The results of the first part of the study are complicated by the use of two significantly different forms of reinforcement, woven roving and 181 style fine woven fabric. Comparisons between different fibers are difficult for this reason, but they are possible since both types of reinforcement were employed in the case of E-glass. Thus, other fibers first are rated relative to E-glass, and subsequently, to each other. This procedure assumes that the ranking of fibers would be the same

regardless of the style of reinforcement, an assumption which is not firmly established.

The ranking of the fibers in order of increasing model composite toughness was LM glass, E-glass, S-glass, Kevlar 49, and Kevlar 29; no consistent difference in interlaminar toughness was observed in comparisons of the various fibers. The effects of matrix and surface treatment were determined by direct comparison of the two values for a single case where all other factors were constant, such as comparing vinylester with polyester for a particular fiber/interface combination. A consistent difference between the two matrices was observed: model composite toughness and average debonding length were greater for the polyester systems in 10 of 12 and 9 of 11 cases, respectively, while the interlaminar toughness was greater for the vinylester in all 12 cases (12 cases are available for comparison since six reinforcements were used including the two styles of E-glass). The effects of surface treatment were less consistent: cleaned surfaces gave higher interlaminar toughness in 9 of 12 cases, but starch-oil gave a higher average debonding length in only 6 of 10 cases, and the model composite toughness results were evenly divided. If only the various glass fibers are considered, then the starch-oil gave a higher average debonding length and model composite toughness in 4 of 6 and 6 of 8 cases, respectively. The Kevlar gave a higher toughness for as-received surfaces in all cases.

The results of the second part of the study indicate that the starch-oil treated laminates are notch-insensitive, while the acetone-cleaned laminates approach notch-insensitivity. This finding suggests that classical fracture mechanics is not valid when normally high fiber volume fractions are used, for cracks propagating perpendicular to the fibers. Thus, while the earlier model composite results may give meaningful trends for low fiber volume fractions, it is the ultimate strength, not the toughness, which controls the fracture of these particular laminates of more common fiber volume fractions.

DISCUSSION

Interpretation of Results

The fracture toughness of fiber reinforced plastic composites is not a property which derives directly from the fiber or matrix toughness and volume fraction, but depends instead upon interactions between the fibers and the matrix [1, 2]. The type of interaction which most directly determines the fracture toughness is the local, subcritical extension of cracks parallel to the fibers at the crack tip [3, 4, 5]. Such cracks may be in the form of a debonding separation propagating along the yarn in the model composite [1] or subcracks and delamination zones in crossplied or woven laminates [4]. Stress transfer across these damage regions is impeded, so the stress tending to cause fiber failure at the crack tip is relaxed [5]. The debonded and cracked regions also serve

to isolate ligaments parallel to the fibers, and the strain energy stored in the ligaments is dissipated upon failure; apparently this energy provides the major contribution to the fracture surface work of composites of this type [1, 2].

While there are strong similarities between the development of the damage zone in the model composite and in woven roving laminates, there are also significant differences which must be considered in the interpretation of the results and in their extension to the projectile impact problem. In the model composite system the debonding of the yarns initiates as the main matrix crack passes the yarn, and propagates along the yarn as the main crack opens [1]. The situation is one of the individual debonded yarns bridging the matrix crack until the yarn is loaded beyond its strength. If the debonded length is longer, then the opening of the main crack imposes a lower average strain on the debonded portion of the yarn than if the same displacement were imposed on a shorter length of the yarn. Thus, a longer debonding length reduces the stress in the yarn for a given crack opening displacement. The strain energy stored in the yarn at fracture also is increased approximately in proportion to the debonded length, thus improving the fracture surface work of the system. The fracture surface work has been found to be proportional to the debonded length for a given system [1].

Therefore, the development of toughness in the model composite is a simple matter of choosing a matrix

and interface which will readily debond, and of choosing a strong fiber with a low modulus to maximize the strain energy stored in the debonded region. The tendency to debond is complicated by a strong dependency on the size and twist of the yarn [1], but the toughness of the model can be optimized for a given yarn such as those taken from 181-style fabric. The optimization of toughness in common types of laminates follows a similar rationale in many cases, but is complicated by additional factors.

The model geometry of isolated, unidirectional yarns, allowed to debond freely until the yarn fails is a characteristic which is not common to higher fiber volume fraction laminates. In fact, if the fiber content of the model were increased beyond a few percent, the crack would not propagate normal to the fibers, but would deflect parallel to them. Such failures are characteristic of unidirectional fiberglass laminates: the crack propagates parallel to the fibers in all cases [6]. The laminates considered in Appendix C were not unidirectional, but were woven roving, with a similar amount of fiber in each principal direction. In this case, the crack originally deflects parallel to the fibers which are oriented normal to the crack, but the adjacent fibers running parallel to the crack constrain this propagation [2]. The eventual damage zone which develops is an arrangement of stable subcracks parallel to the fibers in each direction, but localized to those rovings in the individual layers. At

higher loads, delamination regions may also develop between the rovings and between plies. This type of damage zone is typical for a broad range of fiber reinforced plastics [3, 4].

Damage zones of this type have been shown to have a similar effect to the debonding of yarns in the model in relaxing the high stresses tending to fail the fibers at the crack tip [5], and larger zones result in higher toughness [3]. However, two important aspects of damage zones in laminates are not observed in the model composite: (1) If the damage zone is sufficiently large, the stress concentration may be entirely eliminated so the material is notch insensitive, and (2) the extension of the damage zone is primarily constrained by the neighboring fibers oriented in other directions.

The achievement of a notch-insensitive condition for laminates with fibers oriented in directions such as $\pm 45^\circ$ is common for a variety of composites where the damage zone reaches global proportions in the specimen [4, 7]. It is not so common in $0^\circ/90^\circ$ oriented laminates of E-glass, but apparently was achieved for the laminates in Appendix C due to the starch-oil finish and due to the use of S-glass. E-glass woven roving without starch-oil generally gives notch-sensitive laminates for the $0^\circ/90^\circ$ orientation [7]. The global extension of the subcritical damage zone is closely analogous to the achievement of global yielding in a ductile metal; such laminates may become notch-sensitive if very large specimens are used,

so the damage zone does not spread over the entire specimen.

Some factors which are critical in the development of the damage zone in laminates are not present in the model system. Foremost among these is the resistance to damage zone extension which primarily is a result of the constraint from neighboring fibers oriented in other directions. Thus, thicker plies [3] and coarser fabric weaves [7] lead to larger damage zones and higher toughness. This factor tends to dominate the damage zone development for a given fiber orientation, resulting in a relatively insignificant effect of the type of matrix used [7]. The development of delamination between plies tends to lead to an enlargement of the damage zone, but again the tendency to delaminate in composites is dominated by the reinforcement characteristics [8]. Thus, fiber finish and matrix material are expected to have a limited effect on the fracture toughness of laminates, but what trend there is would be parallel to that in the model system. Additional factors in the case of laminates are the effects of fiber orientation relative to the crack [4], and the effects of modulus on the K-calibration [9] and on the relationship between γ and K_Q [10].

The most prominent feature of the laminates reported in Appendix C is the development of a large damage zone which resulted in notch-insensitive behavior. While the trends observed for variations in fiber/matrix/interface combinations in the model systems (Appendix A) might also have been important in the initial stages of damage zone

development for the laminates, the toughness became inoperative as a criterion of failure as soon as the notch-insensitive condition was achieved. Beyond this point, only those factors influencing the ultimate tensile stress and strain were of significance.

Implications of Projectile Impact

The projectile impact results for the woven roving laminates are discussed in Appendix C. The projectile impact resistance was found to be similar for E and S-glass and similar for each matrix; a consistent improvement was found for the starch-oil treated laminates, although the average improvement was only about 8%. These results do not correlate with the model composite results, where a stronger effect of matrix and fiber than of surface treatment was found, although the general trend with surface treatment is similar. Neither do they correlate with the notched laminate results, which showed little quantitative effect of matrix or surface finish, although a greater degree of notch-insensitivity was observed for the starch-oil treated laminates.

While not studied in this work, the notch-sensitivity of E-glass woven roving laminates with good adhesion has been found to be significant [7], while the present results indicate notch-insensitive behavior for similar S-glass laminates. This difference in behavior of E and S-glass laminates was not observed in the projectile impact tests.

Considering the notch-insensitivity of the tested laminates, it is not surprising that the fracture toughness does not serve as an accurate index of projectile impact resistance. The question still remains as to which easily measured property would be a good index, if any. In this context it is interesting to review the projectile impact phenomenon. A high velocity projectile strikes normal to the surface of the laminate. In passing through the laminate, the projectile causes considerable local damage, including delamination and failure of those fibers near the point of impact.

Several major differences between projectile impact and fracture toughness are evident. First, the criterion for failure is the passage of the projectile through the laminate; this phenomenon does not necessarily require the propagation of opening-mode cracks, although such may occur and may accommodate passage of the projectile. Second, the loading is not similar to that in the fracture toughness tests; those fibers in the path of the projectile are loaded normal to their axis, and no uniform tensile stress field is present around the impact region. Third, the rate of loading is much higher in the case of projectile impact. The most obvious similarity between the two types of loading is that in each case the laminate must distribute locally high stresses and absorb energy to avoid fracture. The types of local damage also appear to be similar in both cases, although projectile impact typically

results in greater delamination between plies. It would seem reasonable to expect that energy absorption in the case of projectile impact would be enhanced if the length over which the fibers are highly strained prior to failure were increased by debonding and delaminating of the fibers over some distance from the point of impact. If so, then this would provide a strong similarity to the fracture toughness tests.

The fracture toughness of laminates does not appear to be an appropriate index of projectile impact resistance because the notch-insensitivity of the particular laminates in question prohibits the determination of a meaningful value of fracture toughness. The energy absorbed in fracturing notched laminates is a function of the specimen size and loading condition because of the global nature of the damage; thus, the fracture energy is not a meaningful parameter when applied to the localized problem of projectile impact. The model composite test does provide a measure of the energy absorbed under localized conditions. However, the model results do not include the effects of high fiber volume fractions, weave effects, or local mode III projectile - composite interaction effects; these may dominate the behavior, so that the parameters operative in the model would fade in significance. An accurate index of projectile impact resistance may require a test which more closely simulates the actual loading, such as a punch test on a region similar in size to the projectile, which

would preserve any interaction between the weave dimensions and the projectile size.

CONCLUSIONS AND RECOMMENDATIONS

Conclusions

Detailed conclusions are presented in the foregoing sections and in the Appendices, and only a few general conclusions will be given here.

1. The fracture surface work of the model composite was sensitive to the type of fiber used. The ranking of the fibers in order of increasing toughness was LM-glass, E-glass, S-glass, Kevlar 49, Kevlar 29. Factors which tended to increase the matrix toughness and interface strength tended to reduce the model toughness but increase interlaminar toughness. Kevlar composites required special techniques for measurement of debonding length, and demonstrated effects of interface treatment different from the glass composites.

2. Fracture toughness tests on woven roving laminates of high fiber volume fraction revealed a consistent notch-insensitive behavior. This is associated with the extension of global subcritical damage zones, and renders the fracture toughness parameters inoperative.

3. Neither type of fracture test employed served as a consistent index of projectile impact resistance. The reasons for this may be related to the simplicity of the model composite, the notch-insensitivity of the woven

roving laminates, and to the inherent differences between opening mode fracture tests and projectile impact tests.

Recommendations

1. The degree of notch-sensitivity of a laminate, while of questionable use in assessing projectile impact behavior, is an important parameter in structural applications. The development of a notch-insensitive condition is very attractive from a structural point of view. The tendency to form large, stable damage zones is important in this regard, and the effects of fiber/matrix interface variables should be studied both experimentally and analytically to elucidate the conditions which lead to notch-insensitivity. Such a study would be possible using existing experimental and analytical techniques.

2. The characteristics of a laminate which lead to optimum projectile impact resistance are not presently known, although certain parallels to fracture toughness behavior are evident. A three-dimensional hybrid-stress finite element analysis has recently been developed with the capability of treating the time-independent aspects of the problem, including the exact modeling of various types of damage at each stage of loading. A combined experimental and analytical study of the parameters influencing impact behavior could lead to a significant improvement in the understanding of the basic aspects of the problem, and could be combined with existing dynamic analyses.

REFERENCES

1. McGarry, F. J. and Mandell, J. F., "Fracture Toughness of Fibrous Glass Reinforced Plastic Composites," Proc. 27th Reinforced Plastics/Composites Div., SPI, (1972) Section 9A.
2. McGarry, F. J., and Mandell, J. F., "Fracture Toughness Studies of Fiber Reinforced Plastic Laminates," Proc. Special Discussion of Solid-Solid Interfaces, Faraday Division of the Chemical Society, Nottingham, England (1972).
3. Mandell, J. F., Wang, S. S., and McGarry, F. J., "The Extension of Crack Tip Damage Zones in Fiber Reinforced Plastic Laminates," J. Comp. Mat'ls. (to be published).
4. Mandell, J. F., McGarry, F. J., Im, J. and Meier, U., "Fiber Orientation, Crack Velocity, and Cyclic Loading Effects on the Mode of Crack Extension in Fiber Reinforced Plastics," Proc. TMS/AIME Conf. on Failure Modes in Composites II, Pittsburgh, Pa. (1974).
5. Wang, S. S., Mandell, J. F., and McGarry, F. J., "Three-Dimensional Crack with Crack Tip Damage in a Crossplied Laminate," presented at ASTM Symposium on Fracture Mechanics of Composites, Gaithersburg, Md. (1974).
6. Hamilton, R. G. and Berg, C. A., "Fracture Mechanics of Fiberglass Laminates," Fiber Sci. & Tech., Vol. 6, 1973, p. 45.
7. Mandell, J. F., McGarry, F. J., Kashiwara, R., and Bishop, W. O., "Engineering Aspects of Fracture Toughness: Fiber/Reinforced Laminates," Proc. 29th Reinf. Plastics/Composites Div., SPI (1974) Section 17D.
8. McKenna, G. B., Mandell, J. F., and McGarry, F. J., "Interlaminar Strength and Toughness of Fiberglass Laminates," Proc. 29th Reinf. Plastics/Composites Div., SPI (1974), Section 13-C.
9. Mandell, J. F., McGarry, F. J., Wang, S. S., and Im, J., "Stress Intensity Factors for Anisotropic Fracture Test Specimens of Several Geometries," J. Comp. Mat'ls., Vol 8 (1974), p 106.

References

10. Sih, G. C., and Liebowitz, H., "Mathematical Theories of Brittle Fracture," in Fracture: An Advanced Treatise, (edited by H. Liebowitz), Vol. 2, Academic Press, New York (1968), p. 67.

APPENDIX A

MODEL COMPOSITE AND INTERLAMINAR TOUGHNESS STUDIES

I. INTRODUCTION

A. General Information

Fiber reinforced composite materials are becoming more and more widely used. Their uses range from high performance aircraft to fishing rods. Most design work in this area is done strictly by empirical methods. Strength criteria and the factors which influence it are fairly straightforward. However, in the area of fracture toughness, much clarification of the factors which affect toughness needs to be done.

Fracture toughness, simply defined, is the resistance displayed by the material to the propagation of a potentially fatal crack. When studying toughness one generally determines either the elastic strain energy release rate with crack growth, G_c , or the critical stress intensity factor, K_{Ic} . The fracture surface work, γ , or the work necessary to form a unit area of crack surface is simply one half of G_c [1].

In composites, analysis is much more involved as one is not working with an isotropic material. However, various studies have confirmed the applicability of fracture mechanics to fiber reinforced systems [2,3,4,5]. Since the fracture toughness of both the fiber and the matrix separately is several orders of magnitude lower than

that of the composite, it stands to reason that the toughness inherent in FRP (fiber reinforced plastics) materials is at least in part due to the interaction of fiber and matrix. Recent research [2,3] points to the energy absorption characteristics of debonded fibers (as the fiber-matrix system is elastically stressed to failure) as a major source of toughness. Let us consider a yarn which has ultimate tensile strength of σ , an elastic modulus of E, and a debonded length of L, then the energy absorbed in the elastic failure of this yarn is, [3]

$$\text{Energy} = L(\sigma^2/2E) \quad (1)$$

When considering the high ultimate tensile strengths of fibers, one can see that this value can be quite significant if the yarns debond individually and have the crack propagating normal to them.

This line of reasoning suggests a number of parameters which may affect the toughness of the composite system. The interfacial region between the fiber and matrix plays an important role. It is the interactions occurring at this interface which determine the amount of debonding which may occur. The quality of the surface finish or size on the fiber should affect the ability of the matrix to bond to the fiber and thus influence the debonding length [6]. Surface finish should also influence the amount of energy required for delamination

of plies in a laminate. Keeping this in mind it was decided to use two types of tests. Both are based on the double cantilever beam technique cited by Berry [7]. Both tests will be described in detail later. The first (model composite double cantilever beam) is meant to approximate a crack propagating normal to the fibers causing debonding and fiber breakage [3]. The other test propagates an interlaminar cleavage crack which it is hoped approximates the delamination phenomena [8]. One can isolate each parameter (i.e. debonding and fracture or delamination) by performing these two tests.

Two different matrices were used in order to eliminate the possibility of artificial trends which are caused by the peculiarities of a particular resin system.

B. Objective of This Study

Due to the importance of fiber/matrix interaction effects, this study attempts to determine what interfacial parameters may be influential in characterizing in-plane and interlaminar toughness behavior.

In the future, correlation between data obtained in this study and high velocity projectile impact research conducted by the U.S. Army Materiel Command will be made.

II. EXPERIMENTAL PROCEDURE

A. Materials and Treatment

As previously mentioned, two matrices were used in this study. The first is Derakane, a vinyl ester manufactured by the Dow Chemical Company. Cure of this matrix was achieved by adding 1.5% by weight of methyl ethyl ketone peroxide (MEK) and 0.25% by weight of 6% Cobalt Napthenate.

The other matrix was Paraplex P-43, a polyester manufactured by Rohm & Haas, Inc. This matrix was cured by adding 0.5% by weight of MEK and 0.8% by weight of 6% Cobalt Napthenate.

In addition to the two matrices, six different fiber/weave combinations were used. (See Figure 1). The woven roving fabric used had a plain weave and weighed approximately 24 ounces per square yard with 5 warp and 4 fill yarns per inch. The fibers used in the woven rovings were E-glass, S-glass, and LM glass. In the 181-style weave, E-glass, PRD49-III, and PRD49-IV were used. The E-glass is found in both fabric styles and thereby provides at least a qualitative comparison between the fabrics. The PRD49-III and PRD49-IV are organic fibers of high strength and modulus made by DuPont and come without a surface finish. The E-glass fabrics came with a commercially applied starch-oil size. The S-glass and LM glass had an epoxy compatible finish (S910). All fabric was

obtained from the U.S. Army Materiel Command with the exception of the two E-glass fabrics. The E-glass woven roving was specially woven by the Bean Fiberglass Company of Jaffrey, N. H. while the 181-style fabric was obtained from Boatex Fiberglass Co. Inc. of Natick, Mass.

To obtain a consistently good finish all the glass fibers were subjected to an acetone bath treatment in order to strip the original starch oil finish off. The bare glass fiber is expected to give relatively good bonding to the matrix in comparison to the starch oil size [6]. The acetone bath consisted of first soaking the fabric in pure acetone for 15 minutes and then rinsing twice again in pure acetone. The PRD49 fibers were not given the acetone bath as they don't have a surface finish.

To get relatively poor fiber/matrix bonding a starch-oil size was applied to all the fabrics except the two E-glass fabrics [6], which were obtained with the commercially applied starch-oil size. The "recipe" for the starch-oil size is listed in Appendix A [9]. After dipping the fabric into the sizing they were hand wrung, spread out, and allowed to dry at room temperature.

During and after treatment all fabrics were handled with gloves or in such a way that body and skin oils did not come in contact with critical areas to reduce the chance of erroneous data.

B. Test Specimen Fabrication

Double Cantilever Beam Model Composite

The double cantilever beam model composite was prepared as follows: two seven-inch long, 3 mm. diameter glass rods were taped parallel to each other, 4 1/2" apart on the surface of a 12 x 12 inch glass plate. This plate had previously been coated with FreKote 33, a release agent manufactured by FreKote, Inc. Yarns taken directly from the treated fabrics were stretched over the rods at 0.1 inch spacings and taped to the plate surface at each end (See Figure 2). A continuous, 0.25 inch thick, one inch wide rubber strip was placed on the plate surface, around three sides of the yarn assemblage. The rubber strip served as both a spacer and a seal. A second glass plate, coated as the first, was placed opposite the first, with the rubber strip separating the two. Spring clips were fastened along the three sealed edges to hold the plates together. The mold was set in an upright position and the matrix material was poured in the unsealed edge at the top through a funnel arrangement.

The matrix was allowed to gel at room temperature (2 1/2 to 4 hours) and then placed in an oven and driven to final cure at 70°C for two hours and then oven cooled.

The following machining was done to bring the specimen to final form. (See Figure 3). The specimens were rough cut on a band saw, yielding three specimens per plate. They were then trimmed to a 1.20 inch width with a high speed router. Two one-eighth inch diameter holes were drilled in one end of the specimen for loading in an Instron testing machine. A slot was then cut along the sides of each specimen to a depth of 0.07 inches with a 0.006 inch thick screw slotting saw on a milling machine. The blade speed was 175 rpm and the feed rate was 1 1/8 inches per minute. A lubricating fluid was sprayed on the blade during cutting to facilitate cutting. The slot was cut completely through the specimen at the loading end to serve as an initial crack. Final dimensions are shown in Figure 3.

After machining, the specimens were subjected to a stress relief and post cure cycle. This consisted of slow heating (2 hours) to 70°C, where the temperature was maintained for 2 hours, and then slow cooling (8 - 10 hours) to room temperature. It is hoped that this procedure insured a full cure and relief from machining stresses.

Double Cantilever Interlaminar Cleavage Specimen

To make the double cantilever interlaminar cleavage specimen it is necessary to make a suitable laminate. The first step is to cut

the material to size. Ordinary household shears were used in cutting the glass fabrics. A Maimin Rotoshere L (H. Maimin Co. Inc.) was used to cut the PRD49 fabrics to a size of 8" x 4". It was found that leaving an inch extra all around the area where the specimens were cut from was the best approach. In this way laminate edge effects such as fiber wash could be eliminated by trimming. The volume fraction of fiber in the laminates was 65%. The laminate thickness was 1/4". Since the fabrics were all slightly different it was necessary to find their unit weight and calculate the correct number of plies to yield the desired laminate. These results are shown in Table 1. Then approximately twice the resin amount calculated is mixed. Layup is then done by hand on a piece of Mylar. The resin is applied equally to each ply. Another sheet of Mylar is placed over it and the layup is then placed in a hot press. Two 1/4" spacers are placed on either side of the layup to control the thickness. The excess matrix is squeezed out with the press (up to 400 psi) and the press is brought up to 70°C to insure curing. It has been found that the addition of heat is necessary as the fabric tends to absorb the heat generated by the exotherm of the resin cure and thus hamper or prevent full cure [10]. The laminate is taken out of the press after two hours.

Machining is done with a diamond circular saw blade mounted on a shaper. The dimensions of the specimen are shown in Figure 4. After machining, $1/4" \times 1/2" \times 1/2"$ aluminum tabs are glued on to the specimen with Epoxi-Patch (Hysol Div., The Dexter Corp.) as shown in the figure. A one to two inch crack is then started between the central plies with a wedge.

Ultimate Strength Specimens

The yarns are obtained in the same manner as for the model composite specimens. They are then dipped in the resin and hung with weights overnight to allow curing. They are then run through a postcure cycle identical to that used for the model composite specimens. The yarns are then cut to $2\ 1/2"$ lengths and globules of epoxy are put on each end to facilitate gripping.

C. Testing and Data Analysis

All testing was done on a standard Instron testing machine with a 1000# load cell.

Cantilever Beam Model Composite

All specimens were pin loaded in tension in the manner shown schematically in Figure 3. The LM-glass specimens did not need any alteration and were tested as received from the postcure cycle. Attempted tests on the remainder of the specimens resulted in improper failure. Because the yarns were too strong vertical cracks would propagate parallel to the yarns through the thickness of the specimen. This effect was counteracted by adhering side reinforcement, in the form of aluminum strips, to the specimen as shown in Figure 5. It has been shown that the addition of side reinforcement does not affect the fracture toughness results [3]. This eliminated the problem in all the specimens with the exception of the S-glass and Paraplex P-43 polyester combinations. However, in these cases, enough data was obtained before vertical cracks nullified the remainder of the data from horizontal crack propagation.

The crosshead rate used for these tests was 0.02 inches per minute while the load scales were 20, 50 or 100 pounds full scale depending on the strength of the yarns.

The crack tip was defined as being the last unbroken yarn which was readily discernable in the presence of cross polarized light (See Figure 6). The twisted yarns failed more distinctly than did the yarns from the woven roving but all were discernable.

The energy absorbed by the advancing crack is taken from the chart by measuring the area involved with a planimeter as shown in Figure 7. This area, A , is inserted into the following equation to yield the fracture surface work, γ :

$$\gamma = A/2wL \quad (2)$$

where $w = 0.08$ inches (the width of the crack) and L is the length of crack over which the energy has been absorbed. The factor of two in the denominator accounts for the two crack surfaces.

The quantity, γ , can be modified by subtracting the contribution from the matrix. The fracture surface work of the matrix, γ_m , was found using the same type specimen as the model composite, the difference being no fibers present. This yields:

$$\gamma' = \gamma - \gamma_m \quad (3)$$

where γ' is the modified fracture surface work.

The final operation which needs to be done on this energy term is a normalization to volume fraction.

This is done as follows:

$$\gamma'' = \gamma' (A_C/10A_Y) \quad (4)$$

where A_C is the area of crack per unit length of crack or 0.08 square inches and A_Y is the area of a yarn of which there are ten per unit length of crack. This value approximates the fracture surface work of 100% volume fraction unidirectional composite which is an imaginary concept. However, this value is useful in estimating the fracture surface work of lesser volume fractions.

Also observed was the debonded length of the yarns. The debonded lengths were measured to the nearest tenth of a millimeter using an eyepiece magnifier, with approximately thirty observations included to yield the average debonded length (ADL). It was not possible to determine a debonded length for the PRD49 yarns using the techniques available. Techniques attempted were microscopic and visual examination under both plain and polarized light, and a fluorescent penetrant dye. In cases where spiral cracking occurred and no debonding was visible, the tip of the spiral crack was used as the end of the debonded length (spiral cracking will be fully explained in the next chapter).

Double Cantilever Interlaminar Cleavage Test

These specimens were pin loaded in the Instron testing machine.

The crosshead rate was 0.2 inches per minute while load scales of 20 and 50 pounds full scale were used. Cracks were monitored visually and reasonable accuracy was maintained (± 0.1 inches).

The Instron output was analyzed with the aid of a planimeter in the same manner as that of the model composite specimens. The data is inserted in the following equation:

$$\gamma_d = A/2wL \quad (5)$$

where γ_d is fracture surface work of delamination, w is the width of the beam and is equal to approximately 0.5 inches, and L is the length of crack over which the energy is absorbed.

Ultimate Tensile Strength

The specimens were loaded in the Instron testing machine and were visually aligned in a set of wedge grips. The crosshead rate was identical to that of the model composite, 0.02 inches per minute. The ultimate load, P , was observed and divided by the cross-sectional area of the yarn to obtain the ultimate tensile strength, σ_{uts} . The area, A_y , was obtained by weighing a 12 inch length of yarn on an analytical balance and using the density for calculations. Four replications of each combination were tested with markedly low values being discarded, as these were thought to be caused by damage during loading.

III. RESULTS AND DISCUSSION

Quantitative results of all testing are presented in comprehensive tabular form in Table 2. This includes averaged results obtained from the double cantilever model composite specimens, the double cantilever interlaminar cleavage specimens, and the ultimate tensile strength specimens. Fracture surface work values of the model composite specimens are given in three forms; as measured, modified, and normalized. Average debonded length is also given. Fracture surface work of delamination values of the interlaminar cleavage specimens are presented and ultimate load and tensile strength as well as area of the yarns are given. Additional tables illustrate selected comparative data.

A. Double Cantilever Beam Model Composite

The range of normalized fracture surface work energies, γ ", was from high values of 3064 and 2100 inch-pounds per square inch (PRD49-IV, as received condition), to low values of 171 and 185 inch-pounds per square inch (LM-glass and Derakane vinyl ester). These values are averaged from three replications and consequently individual specimen values would expand the range somewhat.

In the calculation of these values, the fracture surface work of the matrix, γ_m , used, was 0.37 and 0.16 inch-pounds per

square inch for Derakane vinyl ester and Paraplex P-43 polyester respectively. It is noted that these values are in most cases much smaller (one or two orders of magnitude) than the toughness values obtained for the model composite. It is therefore concluded that the matrix itself contributed very little to the composite toughness.

The resin used did affect the composite toughness, however. It was found that specimens made with Paraplex P-43 polyester gave higher toughness results than those made with Derakane vinyl ester with the exception of the E-glass (from the 181-style fabric) system. This is thought to be due to greater debonded lengths for the polyester systems.

Debonded length is thought to play an important role in the toughness of the composite. In order to examine this hypothesis the stored elastic energy lost upon fracture of the debonded yarn was calculated using Equation 1. The average debonded length, ADL, was used for L and the ultimate tensile strength, σ_{uts} , experimentally measured, was used for σ . The moduli used were 10×10^6 psi for E-glass and 12.7×10^6 for S-glass [6]. These results are compared to measured results in Table 3 and reasonably good agreement is found. Where discrepancies do exist, these are thought to be due to use of experimentally determined ultimate tensile

strength values. The ultimate tensile strength specimens were 2 1/2" long while debonded lengths were of the order of a tenth of an inch. Therefore we would statistically expect that the most serious fatal flaw would occur in the longer length. Examining the data in Table 3 we see that where major discrepancies do exist they are always lower for theoretical values, as would be predicted by the above argument. Previous data, however, have not indicated a strong length-strength dependence in this length range for similar yarns [3].

When the model composite specimens were examined with regard to debonded lengths, several interesting phenomena were noted. In the acetone cleaned S-glass/Paraplex P-43 polyester (SC-P), spiral cracking was found. Spiral cracking, illustrated in Figure 9, occurs as a local stress relieving mechanism. The precise mechanisms are not known, but additional debonding may occur from the tip of the spiral crack. Spiral cracking apparently occurs prior to debonding in fiber/matrix systems where matrix toughness is low, fiber/matrix adhesion is high, and fiber strength is high.

Upon examining the fracture surface of all specimens fabricated with PRD49 yarns it was found that while no debonding could be perceived, tufts of yarn were protruding from the fracture surface

as shown in Figure 10. This did not occur in any of the glass yarn specimens. Opposite surfaces of the fracture were essentially identical, both exhibiting yarn tufts.

Yarn fracture of glass yarns occurred primarily at the matrix fracture surface. Differences were noted between the woven roving yarn fracture and the 181-style yarn fracture. The latter failed as a unit, while the woven roving fibers tended to fail individually. The reason for this was thought to be that debonding of 181-style yarns occurs around the yarn periphery, as shown by Mandell [3], while woven roving yarns debond as separate fibers. This is well demonstrated in the case of LM-glass (starch-oil finish) and Paraplex P-43 polyester (LS-P) where the average debonded length is less than 0.02", but individual fiber debonding was as great as half an inch.

Fracture surface work values are also affected by whether or not the yarn is twisted, since this is the only major difference between the 181-style yarns and woven roving yarns. With the E-glass specimens a direct comparison is possible. Table 4 lists the results of this comparison: in every case the normalized fracture surface work is higher for the 181-style yarns, and the average debonded length (ADL) is also significantly higher in each case. In the light of previous data, it is then inferred that greater debonded

lengths associated with the twisted yarns have caused an increase in toughness.

Perhaps the most striking effects occur with the change of surface finish. In most cases glass yarns exhibited a higher toughness with the starch-oil finish. Here again this is coupled with an increase in debonding length. Therefore, with glass yarns an increase in the debonded length, caused by poorer fiber/matrix adhesion, is thought to be the cause of higher toughness of the model composite specimen.

Just the reverse effect occurred with the PRD49 yarns. In all cases the starch-oil finish caused the fracture surface work to decrease (Table 5). Initially it was thought that the application of the starch-oil size may have in some way caused the ultimate tensile strength of the yarn to decrease. However, upon checking the ultimate tensile strength there was no evidence of this trend. It was then theorized that differences in the degree of matrix impregnation of the yarns might cause the observed effect. Microscopic examination of polished cross sections (polishing done using standard metallurgical techniques) showed no differences. Figure 11 shows such a polished cross section. It is therefore theorized that either the starch-oil finish improves fiber/matrix

adhesion and thereby lessens debonding (unsupported as debonding lengths were not discernible) or some other toughening mechanism is operating.

B. Double Cantilever Interlaminar Cleavage Specimen

The range of fracture surface work of delamination values, γ_d , was 0.45 to 3.27 inch-pounds per square inch. Highest values occurred in the LM-glass/Derakane vinyl ester systems and lowest values occurred in the PRD49-IV (starch-oil finish)/ Paraplex P-43 polyester system.

The most striking trend is that in every case tested the Derakane vinyl ester systems yielded higher fracture surface work of delamination values than the Paraplex P-43 polyester systems. The range of values were 1.42 to 3.27 and 0.45 to 1.84 inch-pounds per square inch for Derakane vinyl ester systems and Paraplex P-43 polyester systems respectively. McKenna [8] found a range of 1.94 to 6.30 inch-pounds per square inch for glass/epoxy systems. The fracture surface work for epoxy is approximately 1.0 inch-pounds per square inch. The trend which then appears to develop is that generally speaking the tougher the matrix, the higher the fracture surface work of delamination, providing good fiber/matrix bonding is established. It must be kept in mind however that this hypothesis has only been made with a limited variety of tests and should be confirmed with other cases.

In most cases the presence of the starch-oil finish lowered the

fracture surface work of delamination. Poorer bonding and thereby a weaker fiber/matrix interface is thought to be the cause.

Upon examination of the specimens, the primary mode of failure appeared to be a fiber/matrix interface failure. The 181-style fabric laminates exhibited double layer delamination (DLD). This is the simultaneous delamination of two adjacent interface regions (Figure 12). This very rarely occurred with the woven roving laminates but nearly always occurred with the 181-style fabric laminates. Values with the 181-style laminates appeared to be slightly lower but this evidence was not conclusive (Table 4).

IV. CONCLUSIONS AND RECOMMENDATIONS

A. Conclusions

The major conclusions of this study are listed as follows:

1. The in-plane fracture toughness of fiber glass composites was found to increase with: (a) weaker fiber/matrix adhesion; (b) higher ultimate tensile strength yarns; (c) twisted yarns rather than yarns from woven roving; and (d) a less tough matrix.
2. The in-plane fracture toughness as measured by the model composite was directly related to the debonded lengths of the glass yarns.
3. The matrix itself contributes very little to in-plane fracture toughness.
4. The PRD49 yarn model composites exhibited lower toughness with the presence of a starch-oil finish on the yarns. Since it was not possible to determine an average debonded length, the toughening mechanism operating was not known.
5. The delamination energy of the laminates increased with increased matrix toughness.
6. The presence of the starch-oil finish on the fibers, thought to decrease fiber/matrix adhesion, lowered the fracture surface work of delamination.

B. Recommendations

1. High velocity projectile impact research should be carried out to define correlations between the energy absorption of the quasi-static testing done in this study and the high rate impact tests.
2. The PRD49 model composite systems should be reinvestigated in order to clearly define the toughening mechanism operating.
3. Further verification of the matrix toughness/fracture surface work of delamination correlation needs to be done.
4. This study should be extended to include ductile matrices as well as other fibers (e.g. boron and graphite).

REFERENCES

1. Tetleman, A. S. and McEvily, A. J., Jr., Fracture of Structural Materials, Wiley, New York, 1967.
2. McGarry, F. J. and Mandell, J. F., "Fracture Mechanisms in a Composite Model", 25th Annual Technical Conference, Reinforced Plastics/Composites Division, SPI, 1970.
3. Mandell, J. F., "Fracture Toughness of Fiber Reinforced Plastics", Ph.D. Thesis, MIT Department of Civil Engineering, June, 1971.
4. Schulz, W. J., et al., "Fracture Toughness of FRP Laminated Plates", MIT, Civil Engineering Research Report R 70-10, 1970.
5. Hiatt, D. B., "Fracture of Prenotched Unidirectional Glass Fiber Reinforced Composites", MIT M.S. Thesis, 1969.
6. Broutman, L. J. and Krock, R. H., Modern Composite Materials, Addison-Wesley, Reading, Mass., 1967.
7. Berry, J. P., "Determination of Fracture Surface Energy by the Cleavage Technique", Journal of Applied Physics, Volume 34, Number 1, 1963, pp. 62 - 68.
8. McKenna, G. B., "Interlaminar Effects in Fiber Reinforced Plastics", M.S. Thesis, MIT Department of Civil Engineering, September 1971.
9. Bohan, C., Picatinny Arsenal, Personal Correspondence, 1972.
10. Bjorksten Research Laboratories, Inc., Polyesters and Their Applications, Reinhold Publishing Corporation, New York, 1960.

APPENDIX A-1

Starch Oil Binder

1. Add 1 1/4 gallons of water* at 110°F (43°C) to bucket.
2. Add 0.95 cc. formic acid.
3. Put 48 cc. of cold water and 4.2 grams of plain gelatin in a paper cup and stir.
4. Take 170 cc. of water out of bucket and put into quart container and stir in 8.45 grams of Elvanol 51.05** (stir and leave aside).
5. Add 1.75 lbs. of corn starch to bucket and break up lumps.
Cook for about 10 to 15 minutes at 160°-180°F (71°-82°C).
6. Immediately add cold water to bring temperature to 160°F (71°C).
7. Add 0.625 cc. of NH₄OH (ammonium hydroxide).
8. Add gelatin dispersion (3) to the bucket.
9. Weigh out 180 grams of unsaturated vegetable oil in beaker and melt on hot plate (if necessary).
10. Weigh out 17.7 grams of Tween #81*** and mix with melted oil.
Add very hot water slowly till container has about 400 cc.
11. Add oil emulsion to the bucket.
12. Add Elvanol (4) to the bucket.
13. Add 4.5 cc. of formaldehyde to the mix.

Starch Oil Binder (Continued)

14. Add water to the 2 1/2 gallon mark in the bucket. Temperature must be higher than 145°F.
15. Keep bucket at 135°F to 145°F (57° - 63°C) during bushing operation.

* Distilled water should be used throughout.

** Polyvinyl Alcohol manufactured by DuPont.

*** Polyoxyethylene sorbitan monooleate manufactured by Atlas
Chemical Industries Inc.

APPENDIX A-2

Specimen Labeling System

General Form: XY - Z

X - Refers to the yarn used in the system

A = E-glass (from 181-style fabric)

E = E-glass (from woven roving)

L = LM-glass

S = S-glass

3 = PRD49-III

4 = PRD49-IV

Y - Refers to the surface treatment on yarn

C = acetone cleaned (or as received condition in the case of the PRD49 yarns)

S = starch-oil size

Z - Refers to the resin used for the matrix

D = Dow Derakane vinyl ester

P = Rohn & Haas Paraplex P-43 polyester

APPENDIX A-3

List of Tables

| <u>Table</u> | | <u>Page</u> |
|--------------|---|-------------|
| 1 | NUMBER OF PLIES OF FABRIC PER LAMINATE | 36 |
| 2 | COMPREHENSIVE TABLE OF RESULTS | 37 |
| 3 | THEORETICAL VERSUS ACTUAL NORMALIZED FRACTURE SURFACE WORK | 40 |
| 4 | E-GLASS: 181-STYLE FABRIC VERSUS WOVEN ROVING | 41 |
| 5 | PRD49: AS RECEIVED CONDITION VERSUS STARCH-OIL FINISH | 42 |

APPENDIX A-4

TABLES

TABLE 1
NUMBER OF PLIES OF FABRIC PER LAMINATE

| Fabric | Number of Plies * |
|----------------------------|-------------------|
| S-Glass woven roving | 14 |
| LM-Glass woven roving | 16 |
| E-Glass woven roving | 13 |
| E-Glass 181-style fabric | 35 |
| PRD49-III 181-style fabric | 33 |
| PRD49-IV 181 style fabric | 33 |

*This pertains to a 1/4" thick 65% fiber volume fraction laminate.

TABLE 2

COMPREHENSIVE TABLE OF RESULTS

| Fiber/Matrix System (a) | γ $\frac{\text{in.-lbs.}}{\text{sq. in.}}$ | γ' $\frac{\text{in.-lbs.}}{\text{sq. in.}}$ | γ'' $\frac{\text{in.-lbs.}}{\text{sq. in.}}$ | γ_d $\frac{\text{in.-lbs.}}{\text{sq. in.}}$ | P lbs. | A_{y-5} 10^{-5} sq. in. | σ_{uts} 10^5 psi | ADL(b) inches |
|----------------------------|--|---|--|--|-----------|-----------------------------------|---------------------------------|------------------|
| LC-P | 1.06 | 0.90 | 200 | 1.70 | -- | 3.6 | -- | 0.04 |
| LC-D | 1.20 | 0.83 | 185 | 3.27 | -- | 3.6 | -- | 0.03 |
| LS-P | 1.16 | 1.00 | 222 | 1.58 | 4.0 | 3.6 | 1.11 | <0.02(c) |
| LS-D | 1.14 | 0.77 | 171 | 3.13 | 4.1 | 3.6 | 1.14 | 0.03 |
| SC-P | 10.37 | 10.21 | 940 | 1.54 | 21.4 | 8.7 | 2.46 | 0.13(d) |
| SC-D | 6.52 | 6.25 | 575 | 2.32 | 23.4 | 8.7 | 2.69 | 0.08 |
| SS-P | 10.20 | 10.04 | 923 | 1.65 | 23.8 | 8.7 | 2.74 | -- |
| SS-D | 8.88 | 8.51 | 783 | 2.10 | 23.0 | 8.7 | 2.64 | 0.10 |
| EC-P | 3.26 | 3.10 | 597 | 1.84 | 9.6 | 4.15 | 2.32 | 0.13 |
| EC-D | 2.78 | 2.41 | 465 | 2.62 | 10.9 | 4.15 | 2.62 | 0.08 |

TABLE 2 (CONTINUED)

| Fiber/Matrix System (a) | γ $\frac{\text{in.}-\text{lbs.}}{\text{sq. in.}}$ | γ' $\frac{\text{in.}-\text{lbs.}}{\text{sq. in.}}$ | γ'' $\frac{\text{in.}-\text{lbs.}}{\text{sq. in.}}$ | γ_d $\frac{\text{in.}-\text{lbs.}}{\text{sq. in.}}$ | P lbs. | A_y 10^{-5} sq. in. | σ_{y5} 10^5 psi | ADL(b) inches |
|----------------------------|---|--|---|---|-----------|-------------------------------|--------------------------------|------------------|
| ES-P | 3.57 | 3.41 | 656 | 1.26 | 13.1 | 4.15 | 3.16 | 0.15 |
| ES-D | 3.74 | 3.37 | 650 | 2.22 | 12.0 | 4.15 | 2.89 | 0.09 |
| AC-P | 3.77 | 3.61 | 705 | 1.07 | -- | 4.10 | -- | 0.18 |
| AC-D | 4.12 | 3.75 | 713 | 2.09 | 13.0 | 4.10 | 3.17 | 0.17 |
| AS-P | 4.45 | 4.29 | 836 | 1.31 | 9.5 | 4.10 | 2.32 | 0.30 |
| AS-D | 5.67 | 5.30 | 1035 | 1.72 | 11.9 | 4.10 | 2.90 | 0.18 |
| 3C-P | 9.82 | 9.66 | 1820 | 1.39 | 19.2 | 4.25 | 4.52 | (e) |
| 3C-D | 8.48 | 8.11 | 1528 | 2.34 | 18.8 | 4.25 | 4.42 | (e) |
| 3S-P | 8.76 | 8.60 | 1620 | 1.40 | 20.1 | 4.25 | 4.73 | (e) |
| 3S-D | 8.08 | 7.71 | 1453 | 1.88 | 19.1 | 4.25 | 4.50 | (e) |

TABLE 2 (CONTINUED)

| Fiber/Matrix System (a) | γ $\frac{\text{in.}-\text{lbs.}}{\text{sq. in.}}$ | γ' $\frac{\text{in.}-\text{lbs.}}{\text{sq. in.}}$ | γ'' $\frac{\text{in.}-\text{lbs.}}{\text{sq. in.}}$ | γ_d $\frac{\text{in.}-\text{lbs.}}{\text{sq. in.}}$ | P lbs. | A_y 10^{-5} sq. in. | σ_{uts} 10^5 psi | ADL(b) inches |
|----------------------------|---|--|---|---|-----------|-------------------------------|---------------------------------|------------------|
| 4C-P | 13.65 | 13.49 | 3064 | 1.35 | 20.6 | 4.40 | 4.60 | (e) |
| 4C-D | 11.94 | 11.57 | 2100 | 2.36 | 17.6 | 4.40 | 4.00 | (e) |
| 4S-P | 10.52 | 10.36 | 1881 | 0.45 | 17.2 | 4.40 | 3.92 | (e) |
| 4S-D | 8.71 | 8.34 | 1519 | 1.42 | 18.7 | 4.40 | 4.25 | (e) |

(a) See Appendix B for Key to Specimen Labeling.

(b) ADL - Average Debonded Length.

(c) Individual fiber debonding was as great as 1/2 inch.

(d) Spiral cracking was present in this case.

(e) No debonding discernible; PRD49 yarn tufts (see Figure 10).

TABLE 3
THEORETICAL VERSUS ACTUAL
NORMALIZED FRACTURE SURFACE WORK

| Fiber/Matrix System (a) | Theoretical γ " in.-lbs./sq. in. | Actual γ " in.-lbs./sq. in. |
|----------------------------|--|---------------------------------------|
| AS-P | 807 | 836 |
| AS-D | 840 | 1035 |
| AC-D | 854 | 713 |
| EC-P | 350 | 597 |
| EC-D | 264 | 465 |
| ES-P | 749 | 656 |
| ES-D | 376 | 650 |
| SC-D | 228 | 575 |
| SS-D | 274 | 783 |
| SC-P | 430 | 1037 (b) |

(a) See Appendix B for Key to Specimen Labeling.

(b) Spiral cracking was present in this case.

TABLE 4

E-GLASS: 181-STYLE FABRIC VERSUS WOVEN ROVING

| Fiber/Matrix System * | γ " in.-lbs./sq. in. | γ d in.-lbs./sq. in. | ADL ** inches |
|--------------------------|--------------------------------|--------------------------------|------------------|
| EC-P | 597 | 1.84 | 0.13 |
| EC-D | 465 | 2.62 | 0.08 |
| ES-P | 656 | 1.26 | 0.15 |
| ES-D | 650 | 2.22 | 0.09 |
| AC-P | 705 | 1.07 | 0.18 |
| AC-D | 713 | 2.09 | 0.17 |
| AS-P | 836 | 1.31 | 0.30 |
| AS-D | 1035 | 1.72 | 0.18 |

* See Appendix B for Key to Specimen Labeling.

** ADL - Average Debonded Length.

TABLE 5

PRD49: AS RECEIVED CONDITION VERSUS STARCH-OIL FINISH

| Fiber/Matrix System* | γ " in.-lbs./sq. in. |
|----------------------|--------------------------------|
| 3C-P | 1820 |
| 3S-P | 1620 |
| 3C-D | 1528 |
| 3S-D | 1453 |
| 4C-P | 3064 |
| 4S-P | 1881 |
| 4C-D | 2100 |
| 4S-D | 1519 |

* See Appendix B for Key to Specimen Labeling.

APPENDIX A-5

List of Figures

| <u>Figure</u> | | <u>Page</u> |
|---------------|---|-------------|
| 1 | COMPARISON OF WEAVES USED IN STUDY | 45 |
| 2 | FABRICATION OF MODEL SPECIMENS | 46 |
| 3 | DOUBLE CANTILEVER MODEL COMPOSITE SPECIMEN | 47 |
| 4 | DOUBLE CANTILEVER INTERLAMINAR CLEAVAGE SPECIMEN | 48 |
| 5 | MODIFIED DOUBLE CANTILEVER MODEL COMPOSITE SPECIMEN | 49 |
| 6 | CRACK TIP REGION IN CROSS-POLARIZED LIGHT SHOWING MATRIX CRACK TIP AT EXTREME RIGHT, FIVE STRESSED YARNS AND THEN TWO BROKEN YARNS TO THE LEFT OF THE MATRIX CRACK TIP | 50 |
| 7 | TYPICAL INSTRON OUTPUT AND ENERGY CALCULATION | 51 |
| 8 | MODEL COMPOSITE SPECIMEN WITH DEBONDED GLASS YARNS IN POLYESTER MATRIX | 52 |
| 9 | SPIRAL CRACKING IN ACETONE CLEANED S-GLASS/ POLYESTER SYSTEM | 53 |
| 10 | PRD49 DEBONDED TUFT PROTRUDING FROM FRACTURE SURFACE. | 54 |
| 11 | CROSS SECTION OF PRD49 YARN IN POLYESTER MATRIX SHOWING MATRIX IMPREGNATION OF YARN | 55 |
| 12 | DOUBLE LAYER DELAMINATION IN LAMINATE CONSTRUCTED FROM 181-STYLE FABRIC | 56 |

APPENDIX A-6

FIGURES

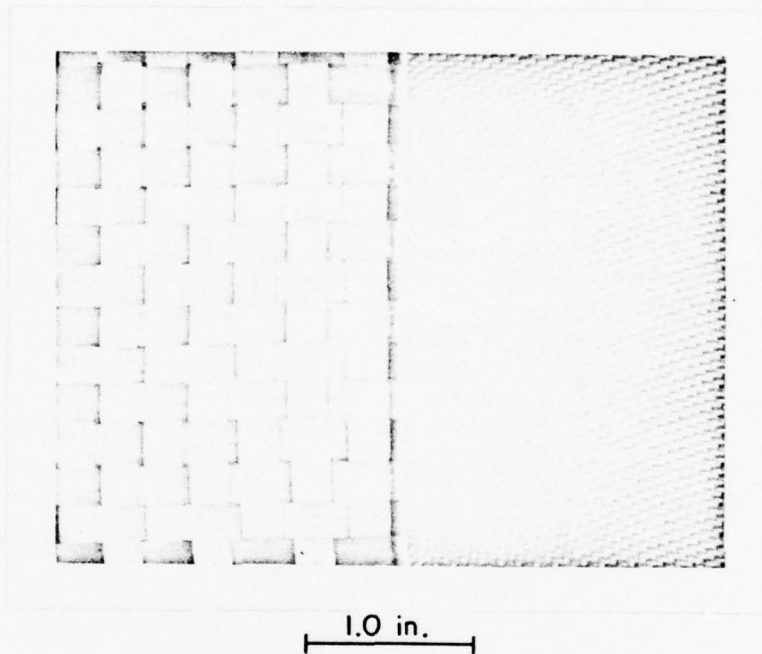


FIGURE 1.
COMPARISON OF WEAVES USED IN STUDY.
Left: 24 oz. Woven Roving.
Right: 181 Style Fabric.

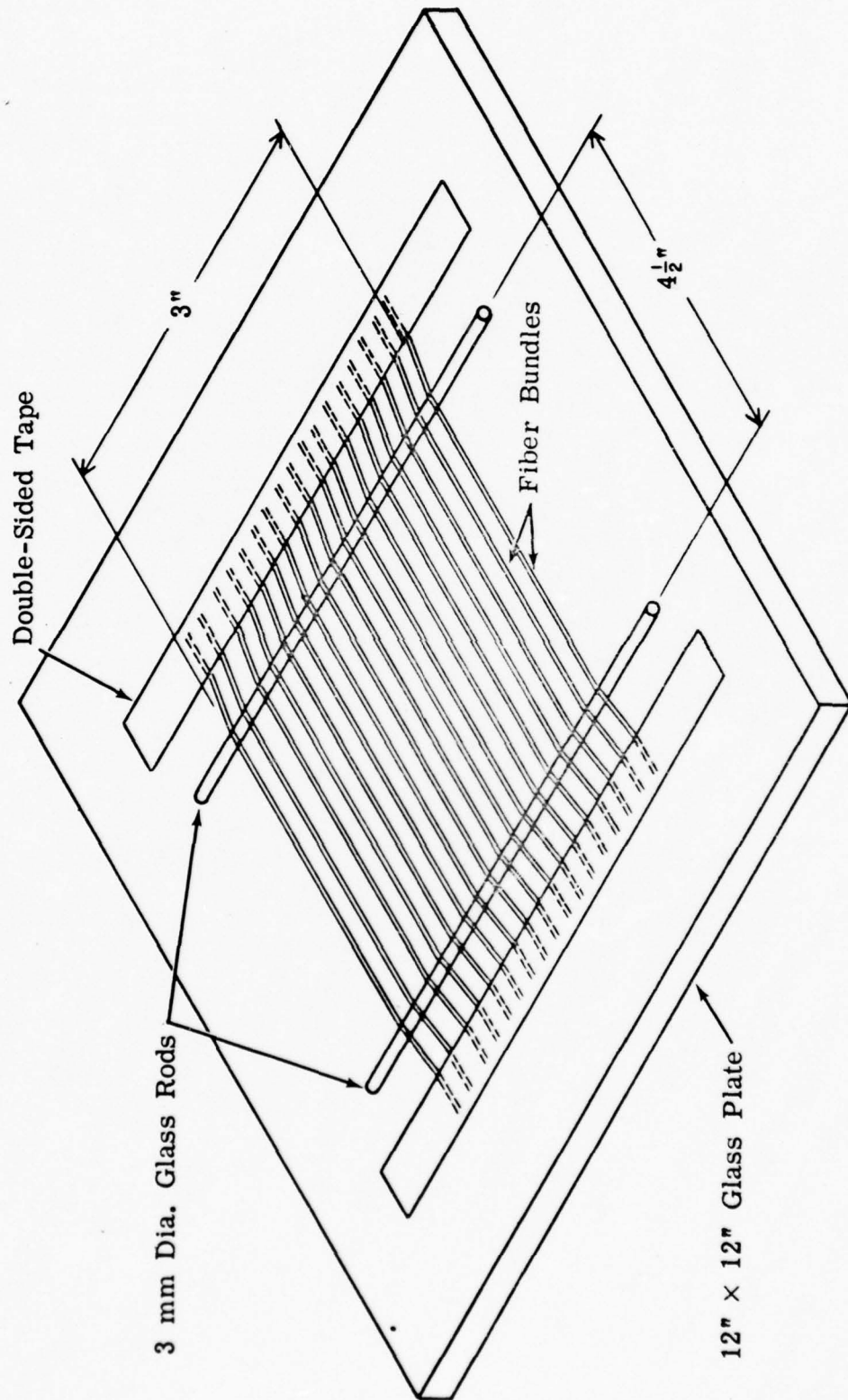


FIGURE 2.
FABRICATION OF MODEL SPECIMENS.

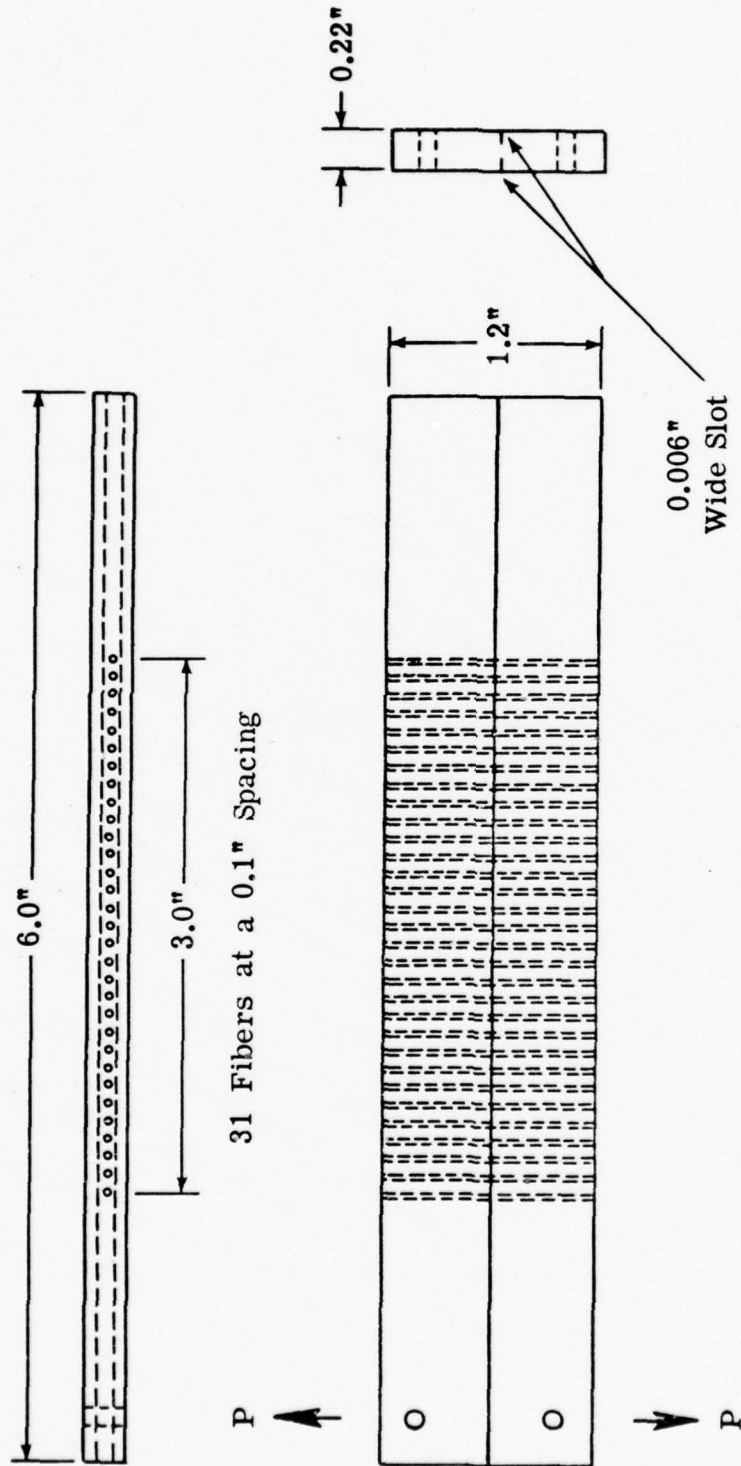


FIGURE 3.
DOUBLE CANTILEVER MODEL COMPOSITE SPECIMEN.

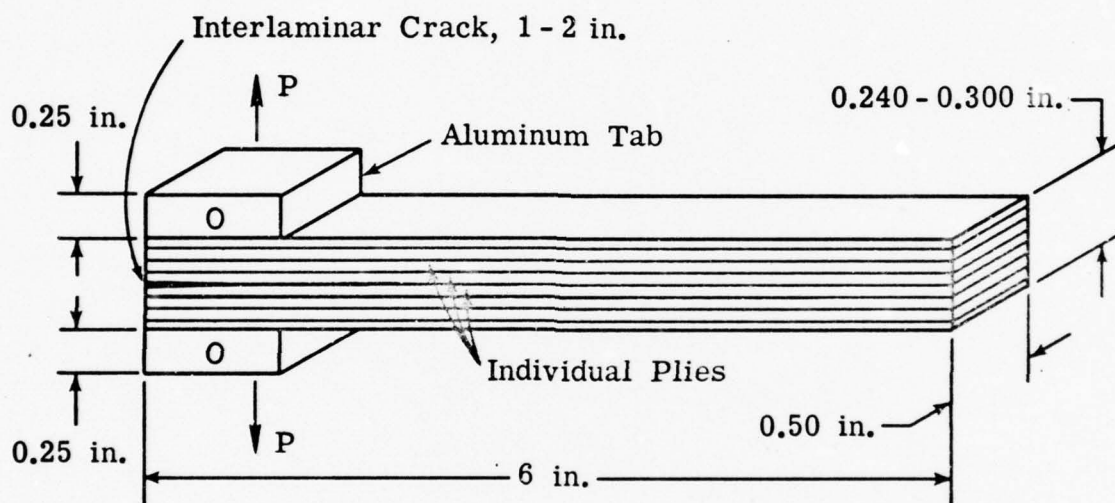


FIGURE 4.
DOUBLE CANTILEVER INTERLAMINAR CLEAVAGE SPECIMEN.

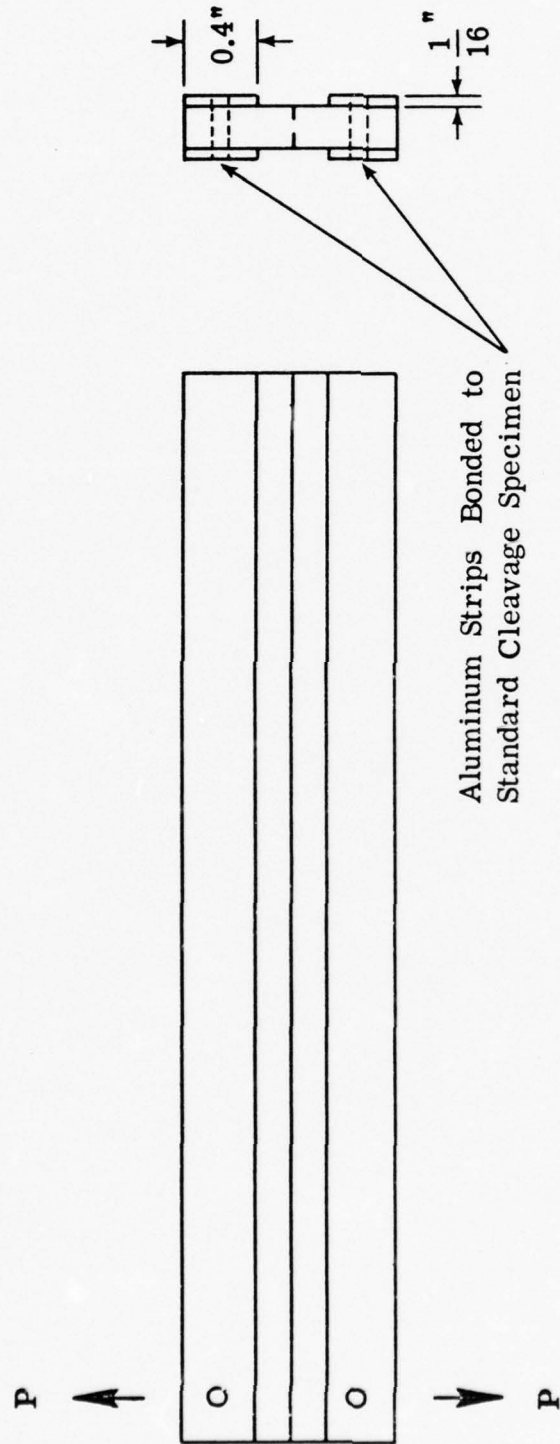


FIGURE 5.
MODIFIED DOUBLE CANTILEVER MODEL COMPOSITE SPECIMEN.

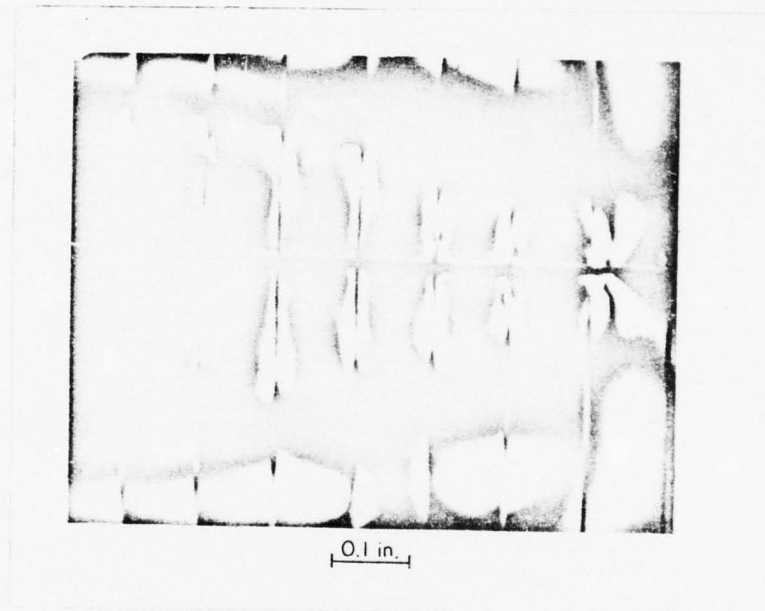


FIGURE 6.
CRACK TIP REGION IN CROSS-POLARIZED LIGHT
SHOWING MATRIX CRACK TIP AT EXTREME RIGHT,
FIVE STRESSED YARNS AND THEN TWO BROKEN
YARNS TO THE LEFT OF THE MATRIX CRACK TIP.

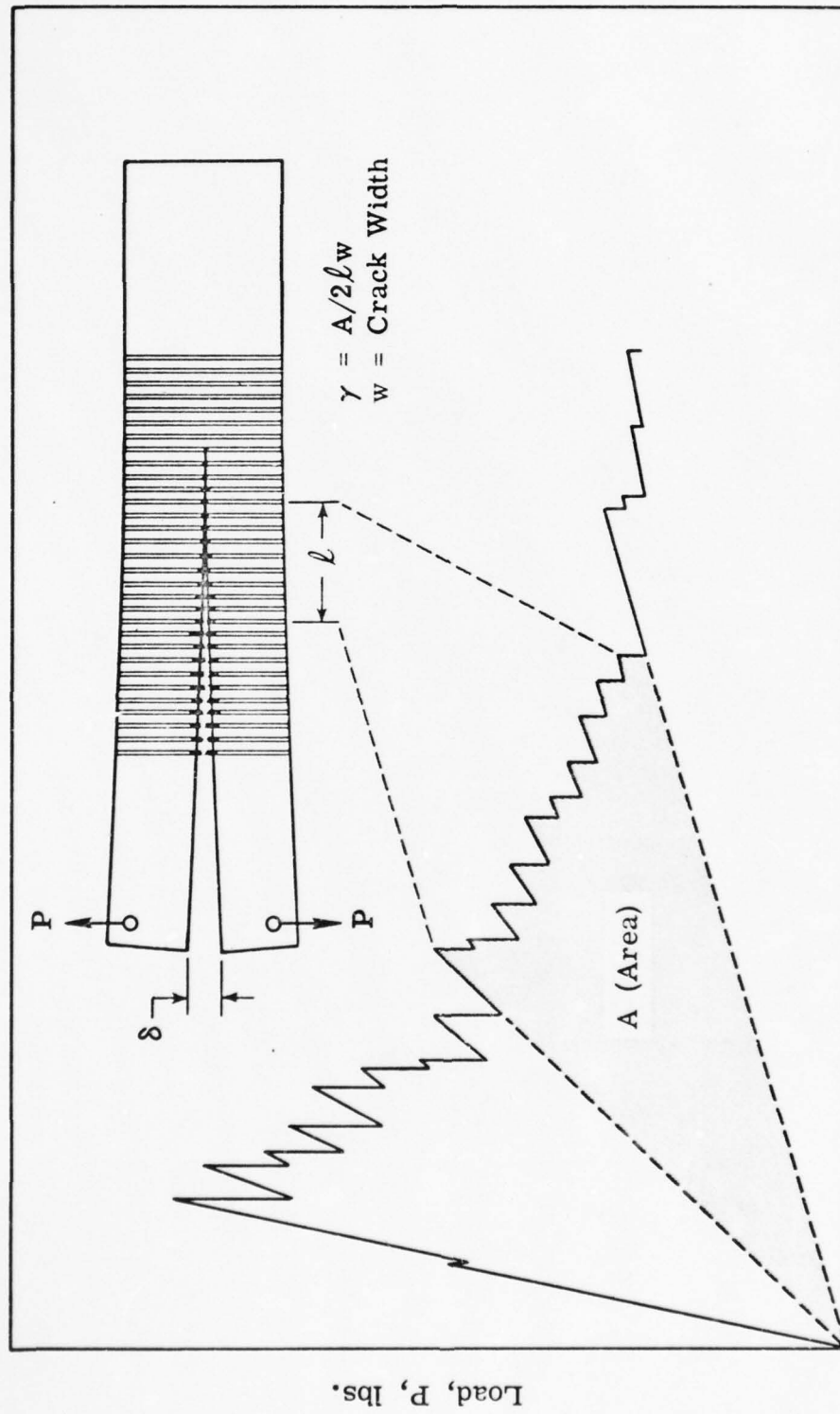


FIGURE 7.
TYPICAL INSTRON OUTPUT AND ENERGY CALCULATION.



FIGURE 8.
MODEL COMPOSITE SPECIMEN WITH DEBONDED
GLASS YARNS IN POLYESTER MATRIX.

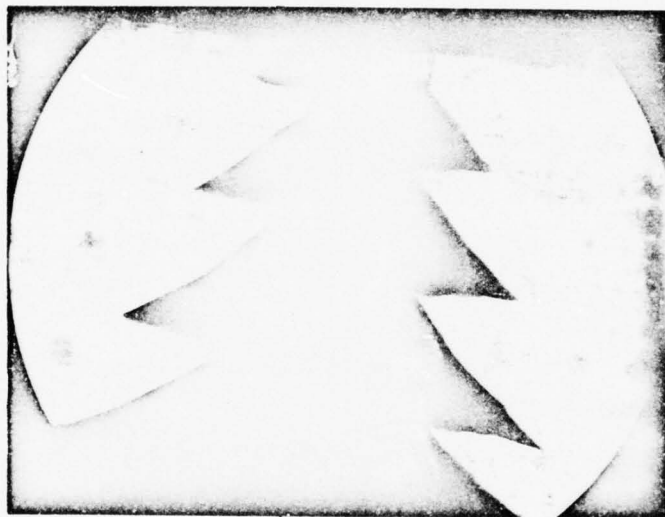
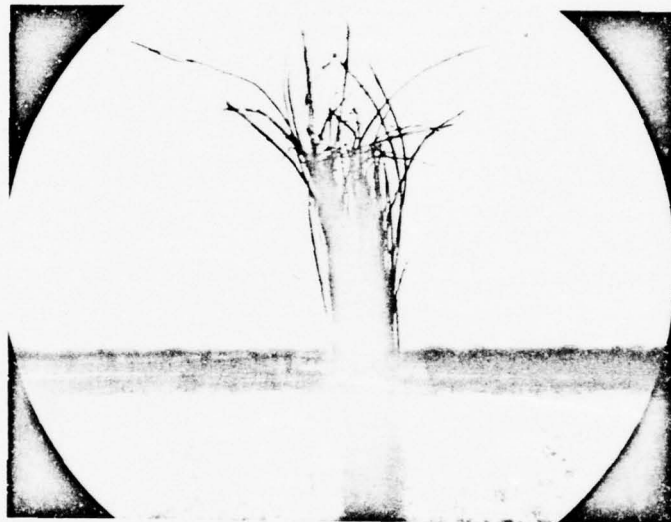


FIGURE 9.
SPIRAL CRACKING IN ACETONE CLEANED
S-GLASS/POLYESTER SYSTEM.



0.02 in.

FIGURE 10.
PRD 49 DEBONDED TUFT PROTRUDING
FROM FRACTURE SURFACE.



0.01 in.

FIGURE 11.
CROSS SECTION OF PRD 49 YARN IN POLYESTER
MATRIX SHOWING MATRIX IMPREGNATION OF YARN.

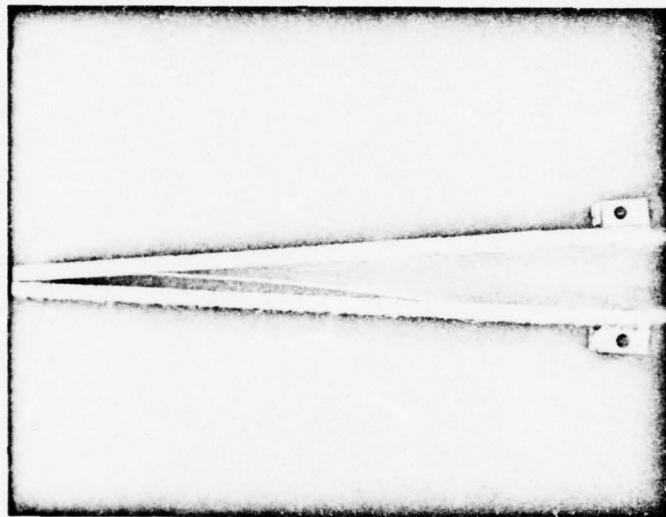


FIGURE 12.
DOUBLE LAYER DELAMINATION IN LAMINATE
CONSTRUCTED FROM 181 STYLE FABRIC.

APPENDIX B

DEBONDING OF KEVLAR COMPOSITES

In Appendix A which describes the initial portion of the program, a problem was encountered in determining the debonding length for the Kevlar fiber model composites. The methods attempted did not reveal any debonding, and some anomalous behavior was observed in that the toughness decreased when starch oil was applied to the fibers, contrary to the results found with other fibers. The debonding problem has been investigated further in the extension of the original work, and some interesting observations are also available from independent studies involving Kevlar composites.

Debonding of Model Composite

The difficulty in determining the debonded length of Kevlar yarns in Appendix A was resolved by use of a more appropriate dye penetrant, Spotcheck Formula B, Type SKL-HF/SKL-S, Magnaflux Corp. This dye decorated the interface region effectively, and the debonding characteristics of the Kevlar yarns proved to be similar in nature and extent to other systems. The data for the average debonding length (ADL) necessary to complete Table 2 of Appendix A is given in the following Table (see Appendix A for a definition of the symbols).

| System | 3C-P | 3C-D | 3S-P | 3S-D | 4C-P | 4C-D | 4S-P | 4S-D |
|----------|------|------|------|------|------|------|------|------|
| ADL (in) | 0.14 | 0.12 | 0.25 | 0.26 | 0.46 | 0.38 | 0.39 | 0.25 |

The peculiar results given in Appendix A which indicated a higher toughness for the clean fibers than for the starch oil treated fibers are now more understandable, particularly for the type IV fiber. It was the Type IV fiber which showed a significantly higher toughness for the cleaned fibers, and the data given above confirms that the debonding length is significantly greater for the cleaned fibers (4C-P and 4C-D) than for the starch oil treated fibers (4S-P and 4S-D). The type III fiber was only slightly tougher when cleaned, and the above data indicate a reversal to shorter debonding lengths for the cleaned fiber, inconsistent with the usual observation of higher toughness with greater debonding length.

The reasons for the shorter debonding length in the case of the starch oil treated type IV fiber are not clear, but may relate either to changes in the tightness of the yarn introduced by the starch oil treatment or to the relatively high strain to failure and slight yielding of this fiber, which would tend to alter the usual debonding characteristics from those of the normal, brittle fibers. The reason that the shorter debonding length of the cleaned type IV fiber does not result in a lower toughness are also unclear. It is possible in both of the above cases that the starch oil may affect the strain to failure of the fiber, but this was not studied directly. If the ductility of the fiber is significant, then the toughness expected from the composite may not follow the theory described in Appendix A.

Fracture Toughness of Kevlar Laminates

As discussed earlier and in Appendix C, the fracture toughness of a laminate depends upon other factors in addition to those dominant in the model composite. In particular, for a 0/90 or woven fabric laminate, the toughness is dependent on the growth of a damage zone at the crack which plays an analogous role to the debonding region in the model composite. The extension of the damage zone is dependent on geometric factors such as the ply thickness or coarseness of weave, and material properties such as shear modulus, interlaminar strength, and fiber strength and failure strain.

Fracture toughness studies have been conducted on 0/90 unidirectional ply and 181-style woven fabric laminates as described in Air Force Materials Lab Report AFML-TR-74-167. The results indicate that the Kevlar laminates show a significantly higher value of fracture toughness than E-glass laminates in all cases tested. Unfortunately, the Kevlar fiber has not been available in woven roving which could be compared directly with other materials in Appendix C or in ballistic tests. The available evidence does suggest that Kevlar would be a likely candidate for good impact resistance.

APPENDIX C

FRACTURE TOUGHNESS OF NOTCHED LAMINATE SPECIMENS

I. INTRODUCTION

At the conclusion of the first part of the study, described in Appendix A, projectile impact tests were run on a number of the laminates by Roylance, et al. [1]. The results indicated that the projectile impact resistance of two systems, S-glass and E-glass woven roving with starch-oil size and the polyester matrix gave the greatest impact resistance; two other systems, S-glass woven roving, acetone cleaned, with polyester and vinylester matrices gave the least resistance. The purpose of the work described in this Appendix was to investigate the fracture characteristics of these four systems using notched tensile tests on laminates of realistic fiber volume fraction. The reason for the additional work was that the tests on the model system described in Appendix A may not reflect all of the important variables which determine the toughness of realistic composites [2].

II. EXPERIMENTAL PROCEDURE

A. Materials

The following are the principal materials investigated in this study:

1. Fibrous Glass Fabric

- a. S-glass: It was a woven roving fabric with a plain weave. It weighed approximately 18 ounces per square yard. The fabric had 5.3 warp and 6 fill yarns per inch. It was supplied by Ferro Corporation, Fiberglass Division of Nashville, Tennessee with an epoxy compatible finish.
- b. E-glass: It was a woven roving fabric with a plain weave. It weighed approximately 18 ounces per square yard. The fabric had 4 warp and 4 fill yarns per inch. It was supplied by Boatex Fiberglass Company, Inc. of Natick, Massachusetts, with an epoxy compatible finish.

2. Resins

- a. Paraplex P-43: A polyester manufactured by Rohm & Haas, Inc. This resin matrix was cured by adding 0.5% by weight of methyl ethyl ketone peroxide (MEK) and 0.8% by weight of 6% Cobalt Napthenate.
- b. Derakane 411-45: A vinylester manufactured by Dow Chemical USA. This resin matrix was cured by adding 1.5% by weight of MEK and 0.25% by weight of 6% Cobalt Napthenate.

B. Fabric Preparation

The glass fabrics were cut to size using ordinary household shears. It was found to be beneficial to cut each glass fabric ply about four inches larger (in both directions) than needed. The extra length allowed the trimming off of laminate edge effects such as fiber wash and to allow for material

lost due to machining.

All glass fabrics were subjected to an acetone bath treatment in order to remove the manufacturer's applied finish. Also, the resulting clean fabrics were to be compared with starch-oil treated fabrics as an illustration of the effect of surface treatment.

The acetone cleaning consisted of allowing each fabric to be immersed in a pure acetone bath at room temperature for 15 minutes. This was followed by two rinsings of the fabric with pure acetone; fabrics were then laid flat and dried.

Glass fabrics were starch-oil treated so that a relatively poor fiber/matrix bond could be obtained. The procedure of Appendix A was used for making the starch-oil bath, and is given in Appendix A-1. Each fabric was dipped into the bath, taken out and laid on a flat surface. The excess starch-oil was removed by using a household roller pin. The fabric was then set aside to allow it to dry at room temperature (while flat).

During and after the surface treatment, all glass fabrics were handled with gloves so that the fabrics would not be contaminated by skin oils, etc.

C. Fabrication of Specimens

There were four different fiber/matrix systems to be tested. They were acetone clean treated S-glass/Derakane, acetone clean treated S-glass/Paraplex, starch-oil treated

S-glass/Paraplex, and starch-oil treated E-glass/Paraplex.

A typical laminate was to be four plies thick with a fiber volume content of 54%. Hence, the ideal laminate thickness was 0.071". The fabrication of a laminate was done by hand layup on a sheet of Mylar. An excess amount of resin matrix was used for the laminate. It was found that three times the amount technically needed was convenient.

The hand layup involved placing and spreading out an equal amount of the prepared resin matrix on both sides of each ply. The plies were all laid in the same direction. Another sheet of Mylar was placed on top of the layup and the assembly was placed in an unheated hot press. Two 0.071" spacers were placed on either side of the layup so as to control the thickness. The hot press was turned on and set for 70°C. Meanwhile, contact pressure was achieved and maintained for five minutes. The pressure was then slowly increased to 400 psi in order to squeeze out the excess matrix. The entire assembly was then allowed to be heated at 70°C for two hours to insure a full cure.

The laminates were machined to specimen shapes illustrated in Fig. 1. The machining entailed making rough cuts with a diamond edge circular saw; the final dimensions were achieved on a Tensilkut router. The notches were made with a 0.018" thick diamond edge wheel. The length of the notch on each side was 0.375 inches.

The machining was done such that the laminates were oriented in the 0° direction; i.e., the fill direction was to be parallel to the load and the warp direction was to be normal to the load.

The shape of the unnotched tension (i.e. UTS) specimen in Fig. 1 was a shape determined by trial and error so as to give the least stress concentration while avoiding grip failures [3].

D. Testing of Specimens

All tests were conducted on an Instron Universal testing machine at room temperature and humidity with a 10,000 pound load cell. The displacement rate was 0.2 inches per minute. All specimens were loaded by 2 inch wide wedge-action grips. The replication factor for the UTS specimens was three except in the case of the starch-oil E-glass/Paraplex system where it was two. The replication factor for the notched tension (i.e., DEN) specimens was at least five for all cases. Values of K_Q , net strength, and ultimate tensile strength were calculated as in previous studies [3]. The calculation for K_Q includes a geometric calibration factor, Y , as

$$K_Q = \sigma Y \sqrt{c} \quad [1]$$

The isotropic value for Y was used in all cases, which introduces a small error as discussed in [3].

III. RESULTS AND DISCUSSION

The quantitative results of the various tests are listed in tabular form in Appendix C-1. The average normalized values of the net fracture strength (σ'_{net}) and the candidate fracture toughness (K_Q), derived from the double-edge-notched (DEN) specimens and the ultimate tensile strength (σ'_{uts}) from the UTS specimens, are given in the table. Also shown, are the representative maximum load (P_{max}) and the fiber volume content (V_f) values for each group of specimens. In most cases, the load-deflection curves were linear with a small amount of inelastic behavior occurring just prior to failure. The load used in calculating K_Q (also σ'_{net}) and σ'_{uts} was the average peak value for each group of specimens.

For all specimens tested, there was no failure in the grips. However, there were some cases where failure occurred in the transitional area of the UTS specimens.

In Appendix A, 13 or 14-ply laminates (depending on the fabric) were used in the experiments. It was found that it was necessary to employ 4-ply laminates in the present work. However, it has been reported by Mandell et al. [3], that for a range of laminate thicknesses (which covers both Appendix A and the present work), varying the laminate thickness has a negligible effect on the fracture toughness. Further, the modified numbers in Appendix C-1 have been normalized to the average fiber volume fraction of 54%.

The normalized numbers σ'_f , σ'_{net} and σ'_{uts} were determined by multiplying the gross fracture stress (σ_f), σ_{net} and σ_{uts} by the ratio of the new fiber volume content (0.54) to the fiber volume content of the laminate of interest ($0.54/V_f$). The normalized fracture toughness (K'_Q) was derived from Eq. 1 by substituting K_Q and σ_f with K'_Q and σ'_f respectively. McGarry and Mandell [4] showed that K_Q and σ_{uts} are generally proportional to the fiber volume fraction. Hence normalizing the numbers should have a minimal, if any, effect on the true relationship between the various laminates.

A. Double-Edge-Notched Specimens

The range of normalized values for the three S-glass laminates is quite narrow. The differences are small enough such that no trend can be determined. In Fig. 2, a typical load-deflection curve for an S-glass composite is given. The composite is essentially elastic during most of the loading. However, it does experience inelastic behavior just prior to failure. The linear response of the graph shows that the effect of fiber/matrix debonding and delamination (examples of inelastic behavior) is quite small.

In comparison to the S-glass, the E-glass laminates show remarkably lower values for strength and toughness. Normally, the strength of S-glass laminates are about 30% to 40% greater than similarly made E-glass laminates [5].

However, the difference here is about 300%. This large difference can be partially explained in Figs. 3, 4, and 5. Figure 3 shows both glass fabrics before surface treatment and Figs. 4 and 5 show the final result of handling during the surface treatments of S-glass and E-glass respectively. Because of its tighter weave, S-glass tolerated the handling much better than E-glass. The misorientation of yarns in a laminate has been reported by Mandell et al. [6] as to significantly lower the strength and fracture toughness of the laminate. The apparent explanation is that when a specimen is loaded under tension, the yarns try to orient themselves toward the stress. The resultant delamination is analogous to the ones experienced by $+45^\circ/-45^\circ$ laminates [6]. This delamination is an important fracture mechanism and is illustrated by the inelastic behavior of the load-deflection curve of a typical E-glass specimen (Fig. 2).

The effect on the fracture toughness by choice of fiber has been reported (Appendix A). Using a model composite system to show that the fracture surface work for E-glass laminates was much less than that for S-glass. These results also agree with this work on the insignificant effect that the starch-oil size and the choice of resin matrix has on the normalized fracture toughness.

Although a model composite system was used in the previous work, and quantitative correlation with laminates of much higher fiber volume content would be unexpected, trends can

observed and are expected to be applicable to higher fiber volume content laminates, since the mechanisms of crack resistance are similar [4].

Roylance et al. [1] reported that in all cases treated, the use of a starch-oil size resulted in an increase in ballistic impact strength. However, there was only an average of 8% improvement. Although this relatively small improvement may be significant in actual applications, it would be difficult to achieve good correlation with the ultimate tensile strength and fracture toughness values, even if such a correlation did, in fact, exist. This difficulty can be reflected by the proportionality of the kinetic energy of the " V_{50} " projectile to the fracture energy of the specimen. The " V_{50} " projectile represents the velocity for which a projectile would have a 50% probability of completely penetrating the target specimen.

Assuming the target specimen to be an elastic material, the energy lost by the bullet (E) on impact, is assumed to be related to the candidate critical strain energy release rate (G_Q).

$$G_Q \propto E \quad (2)$$

This leads to

$$G_Q \propto 1/2 mv^2 \quad (3)$$

where m is the mass and v is the velocity of the projectile in the ballistic test.

For an isotropic material [7]:

$$G_Q = \frac{K_Q^2}{M} \quad [4]$$

where K_Q is the candidate critical stress intensity factor (fracture toughness) and M is the Young's modulus.

From Eqs. 3 and 4:

$$\frac{K_Q^2}{M} \propto 1/2 m v^2 \quad [5]$$

From Eqs. 1 and 5:

$$\frac{\sigma_f^2 Y^2 c}{M} \propto 1/2 m v^2 \quad [6]$$

From the above, the velocity of the "V₅₀" bullet is directly proportional to the strength and fracture toughness of the material. Hence, the 8% difference can be applied to the strength and fracture toughness results of the DEN specimens. However, the typical scatter for the values here are about 10%. Therefore, even if fracture mechanics were valid and directly related to the ballistic impact resistance, valid correlation would still be difficult to establish.

The ballistic results, when compared to Appendix A and to this work, agree that neither resin, Derakane or Paraplex

yielded laminates with a higher fracture toughness than the other. However, contrary to both parts of the present study, E-glass achieved similar impact results with S-glass, and starch-oil was found to give consistently improved performance.

B. Ultimate Tensile Strength Specimens

The considerable amount of difference between the normalized ultimate tensile strengths of the E-glass and S-glass laminates could be attributed to the same reasons as given for the low values of normalized net fracture stress and fracture toughness from the starch-oil treated S-glass/Paraplex laminates.

Taking the S-glass laminates as a group, there was an insignificant difference in normalized ultimate tensile strengths between laminates made with different resins. However, there was a significant decrease in normalized ultimate tensile strength in the case of the starch-oil treated S-glass/Paraplex laminate.

Observations of the actual specimens show that the acetone clean treated laminates suffered much less inter-laminar failure than the starch-oil treated laminates. In Fig. 6, examples of UTS specimens which have been tested are shown for the two starch-oil treated and the acetone clean treated S-glass/Paraplex laminates (the two acetone cleaned cases failed in a singular fashion).

A trend illustrating a difference between two surface treatments can be seen upon comparing the normalized ultimate tensile strength to the corresponding normalized net fracture stress. For the starch-oil treated laminates, the normalized ultimate tensile strength was lower than the corresponding normalized net fracture stress. The opposite was true for the acetone clean treated laminates.

It is apparent that the relatively larger amount of delamination of the starch-oil treated laminates resulted in lower normalized ultimate tensile strength (which becomes an additional factor in causing the very low normalized ultimate tensile strength of the E-glass laminate). Hence, delamination is an important fracture mechanism in addition to the fiber fracture which predominates in acetone clean treated laminates.

The reason that DEN specimens from the starch-oil treated S-glass/Paraplex laminate did not have relatively lower normalized net fracture stresses (hence indicating delamination was not the principal fracture mechanism), was because the notches acted to constrain the delamination to an area between the two notches of the specimen, avoiding free-edge effects. This constraint on delamination can be seen in Figs. 7 and 8. The two acetone clean treated laminates showed similar results, so a representative specimen is shown in Fig. 7. The whitened area shows the delaminated area of the specimen. At fracture, the delamination did finally

extend to the edges of the specimen, but only to a small degree. The actual starch-oil treated S-glass/Paraplex specimens showed more interlaminar separation than the acetone clean case, but most of the delamination did not occur until late in the loading cycle, extending to the edges of the specimen. Until then, most of the delamination occurred in the area between the notches as seen in Fig. 8.

Interlaminar separation was quite obvious for the case of the starch-oil treated E-glass/Paraplex laminate. As can be seen in Fig. 9, the notches did act to constrain the delamination somewhat. But due to the degree of delamination that eventually occurred, it is questionable whether the low values for the E-glass laminate were the result of delamination or fiber fracture being the primary fracture mechanism; perhaps it was a combination of both. However, the added parameter given by the inherent misorientation in the laminate adds more doubt to the reliability of the E-glass results.

C. Validity of Fracture Mechanics

Up to now, it has been assumed that fracture mechanics was valid for the fiber/matrix systems examined in this work. However, taking the ratio of σ'_{net} to σ'_{uts} (see Appendix C-1), the laminates with plies treated with starch-oil are clearly notch insensitive and the laminates with plies cleaned with acetone are nearly so.

Technically, the acetone clean treated laminates are not notch-insensitive. However, Srawley and Brown (26) reported that the A.S.T.M. Special Committee on Fracture Testing had suggested that for metals, fracture mechanics would be sufficiently valid only if a criterion was met. This criterion was that the net fracture stress should be less than 80% of the uniaxial yield strength.

Although this was for metals, it provides a guide if the material is elastic and isotropic. Assuming the composite behaves fairly elastically up to the maximum load in the UTS tests, then the ultimate tensile strength could be substituted for the uniaxial yield strength.

In the case of the acetone clean treated laminates, upon comparing the ratios (normalized net fracture stress to the ultimate strength) to the criterion, shows that for these particular laminates, fracture mechanics is essentially invalid.

Knowing that the materials tested are notch insensitive, the calculated values of the fracture toughness (K_Q) are now inoperative.

An interesting analogy can be made between this work and work done by Mandell et al. [6] on graphite/epoxy laminates. Notch sensitivity of the material was dependent on the size of the damage zone at the original crack tip. For a $+45^\circ/-45^\circ$ graphite/epoxy laminate, the damage zone was found to have extended through the entire width of the

specimen just prior to fracture. The resulting stress gives a net fracture stress approximately equal to the ultimate strength.

In the cases tested here on glass woven roving, the extension of the damage zone and the resulting notch insensitivity lends credence to the analogy.

Mandell et al. [6] shows that increasing the width of the specimen does not affect the ratio of net fracture stress to ultimate strength for the $+45^\circ/-45^\circ$ laminates. But increasing the width causes the ratio to decrease for other laminates employing 0° and 90° plies. Perhaps, from the analogy, the fiber/matrix systems tested here are unaffected by specimen width.

When fracture toughness tests are run, a meaningful value for K_Q can be obtained only if the radius of the notch is below the critical value (ρ_0). A blunt crack can result in an erroneous K_Q and, hence, failure of fracture mechanics. Mandell et al. [3] reported a value of 0.1 inches for the critical radius. The radius of the notch used here was 0.009 inches, which easily meets that criterion.

The validity of fracture mechanics with respect to Roylance's results [1] is now in question. Knowing that fracture mechanics is not valid for the fiber/matrix systems tested here, it would seem reasonable to assume that fracture mechanics is not valid for similar fiber/matrix systems in Roylance's work.

With the high rates of loading achieved in ballistics tests, it is expected that the target specimen as a whole would become even more notch insensitive [3]. However, since the loading conditions are different from those in DEN specimens, notch sensitivity might exist. The projectile, upon impact, might only create a relatively small damage zone which may not be large enough to relieve the stress concentrations (i.e., to blunt the cracks). The inability to relieve the stress concentrations could lead the material to become notch sensitive.

If fracture mechanics was valid for the impact tests, the trends shown by the model composite systems should indicate similar trends in Roylance's results. However, the results on E-glass versus S-glass sharply disagree and this lends more credence to the impact specimens being notch insensitive.

CONCLUSIONS AND RECOMMENDATIONS

A. Conclusions

1. All laminates were notch insensitive under the conditions they were tested.
2. No meaningful correlation could be made with Appendix A results because of the invalidity of fracture mechanics in this work.
3. Fibers coated with a starch-oil size lowered the ultimate tensile strength with a marked increase in inter-laminar separation. Roylance showed an improvement in impact energy absorption due to the presence of the starch-oil.
4. There was no significant difference between the two resins tested with respect to the composite strength. Roylance reports similar results with respect to impact energy absorption.
5. S-glass showed a significantly higher ultimate tensile strength when compared to E-glass while Roylance showed that impact energy absorption was relatively insensitive.

B. Recommendations

1. Tests involving the E-glass laminate should be repeated

but with an industrially applied starch-oil size on the fabric.

2. This study should be expanded to include other fiber/matrix systems not covered here.
3. A study should be done to elucidate the reasons for E-glass laminates to achieve similar impact energy absorption results with S-glass laminates, even though E-glass is inherently weaker than S-glass.
4. Some work should be done to investigate further the analogy between the starch-oil treated laminates and $+45^{\circ}/-45^{\circ}$ unidirectional ply laminates.

AD-A040 388

MASSACHUSETTS INST OF TECH CAMBRIDGE
FIBER/MATRIX INTERACTION EFFECTS ON FRACTURE TOUGHNESS OF STRUC--ETC(U)
JUL 75 D G PIRES, J F MANDELL, C E FONG

F/G 11/4

DAAG46-72-C-0233

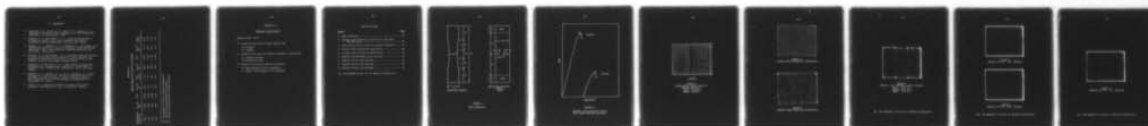
AMMRC-CTR-75-15

NL

UNCLASSIFIED

2 OF 2

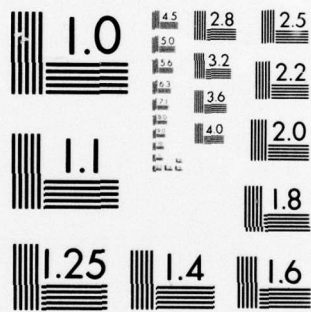
AD
A040388



END

DATE
FILMED

7-77



MICROCOPY RESOLUTION TEST CHART
NATIONAL BUREAU OF STANDARDS-1963-A

V. REFERENCES

1. Roylance, M. E., Pires, D. G., Lewis, W. R., McGarry, F. J., "High Rate Projectile Impact Resistance of Fiber Reinforced Composites," in preparation (1975).
2. McGarry, F. J. and Mandell, J. F., "Fracture Mechanisms in a Composite Model," 25th Annual Technical Conference, Reinforced Plastics/Composites Division, SPI, (1970).
3. Mandell, J. F., McGarry, F. J., Kashiwara, R., and Bishop, W.O., "Engineering Aspects of Fracture Toughness: Fiber Reinforced Laminates," Proc. 29th Reinforced Plastics/Composites Div., SPI (1974), Section 17D.
4. McGarry, F. J. and Mandell, J. F., "Fracture Toughness Studies of Fiber Reinforced Plastic Laminates," Proc. Special Discussion of Solid-Solid Interfaces, Faraday Division of the Chemical Society, Nottingham, England (1972).
5. Lindsay, E. M. and Hood, J. C., "Final Report on Glass Reinforcements for Filament Wound Composites," Owens-Corning Fiberglas Corp., TR-63-8-104, Contract No. AF 33 (657)-9623 (1963).
6. Mandell, J. F., McGarry, F. J., Im, J. and Meier, U., "Fiber Orientation, Crack Velocity and Cyclic Loading Effects on the Mode of Crack Extension in Fiber Reinforced Plastics," Proc. TMS/AIME Conf. on Failure Modes in Composites II, Pittsburgh, Pa. (1974).
7. Irwin, G. R., "Analytical Aspects of Crack Stress Field Problems," TAM Report 213, Univ. of Illinois, (1962).

APPENDIX C-1

TABULAR RESULTS FOR DEN AND UTS SPECIMENS

| Fiber/Matrix System (a) | P_{\max} (b) lbs. | V_f (b) | σ'_{net} (b) ksi | K'_Q (b) ksi $\sqrt{\text{in}}$ | P_{\max} (c) lbs. | V_f (c) | σ'_{uts} (c) ksi | $\frac{\sigma'_{\text{net}}}{\sigma'_{\text{uts}}}$ |
|----------------------------|---------------------------|--------------|--------------------------------------|---|---------------------------|--------------|--------------------------------------|---|
| SC-D | 6290 | 0.634 | 70.3 | 53.7 | 8080 | 0.595 | 75.2 | 0.93 |
| SC-P | 6600 | 0.595 | 73.7 | 56.4 | 8650 | 0.586 | 80.5 | 0.92 |
| SS-P | 6440 | 0.509 | 72.0 | 55.0 | 6900 | 0.516 | 64.2 | 1.12 |
| ES-P | 2300 | 0.533 | 26.2 | 20.1 | 2230 | 0.533 | 21.2 | 1.24 |

(a) See Appendix C for key to specimen nomenclature.

(b) Values for Double-Edge-Notched specimens.

(c) Values for Ultimate Tensile Strength specimens.

APPENDIX C-2

Specimen Nomenclature

General Form: XY-Z

X - refers to the type of glass fabric used

E = E-glass

S = S-glass

Y - refers to the type of surface treatment on the fabric

C = acetone cleaned

S = starch-oil size

Z - refers to the resin used for the matrix

D = Dow Derakane 411-45 vinylester

P = Rohm & Haas Paraplex P-43 polyester

LIST OF FIGURES

| <u>Figure</u> | <u>Page</u> |
|---|-------------|
| 1. Test Specimens..... | 35 |
| 2. Typical Load Deflection Curves for 2 Inch Wide DEN Specimens..... | 36 |
| 3. Woven Roving Fabric Prior to Surface Treatment..... | 37 |
| 4. S-Glass after Starch-Oil Application..... | 38 |
| 5. E-Glass after Starch-Oil Application..... | 38 |
| 6. Typical UTS Specimens after Fracture..... | 39 |
| 7. Typical SC-P(a) DEN Specimen..... | 40 |
| 8. Typical SS-P(a) DEN Specimen..... | 40 |
| 9. Typical ES-P(a) DEN Specimen..... | 41 |

(a) See Appendix C-2 for key to specimen nomenclature.

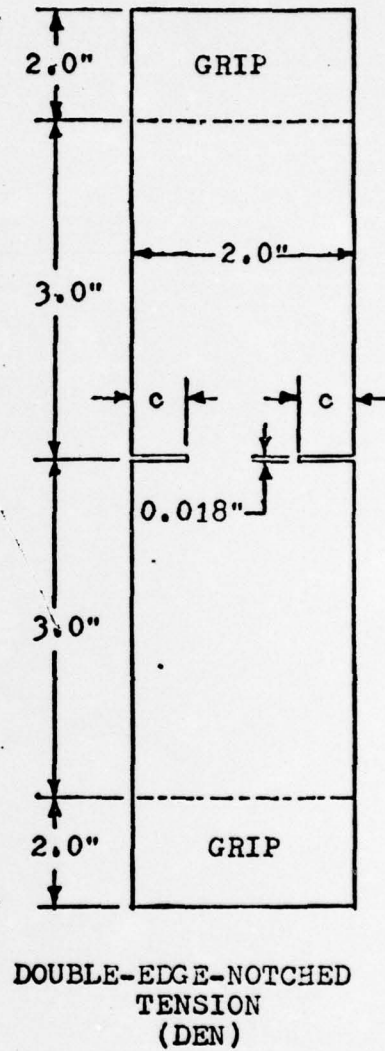
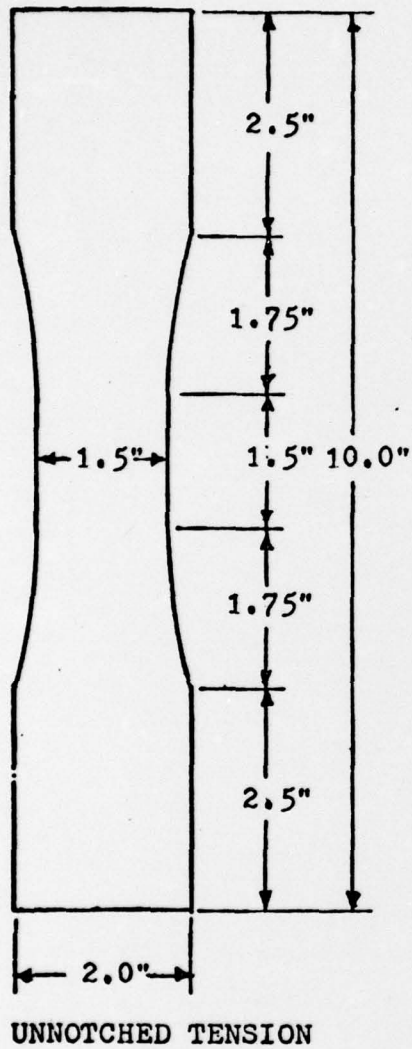


FIGURE 1.
TEST SPECIMENS.

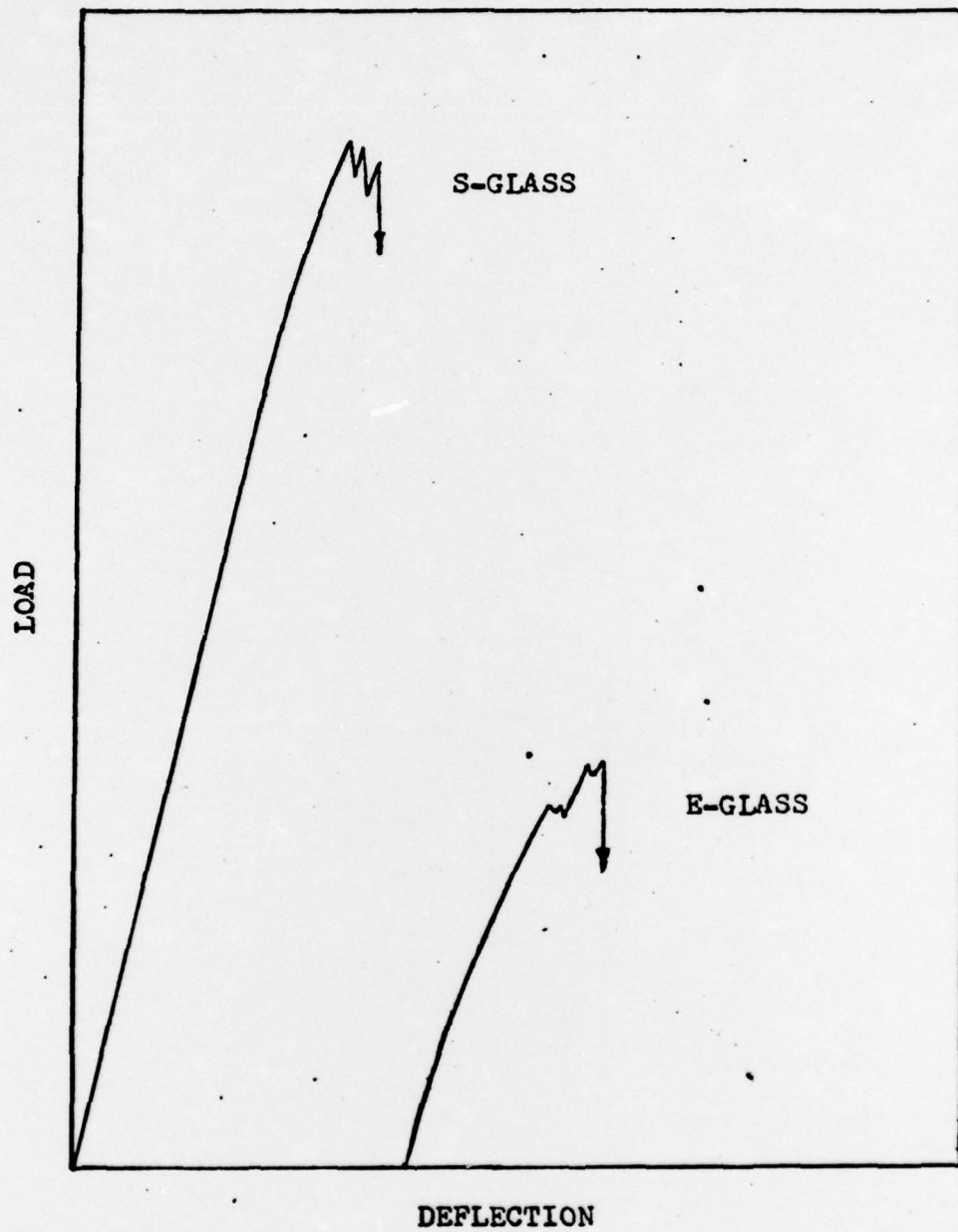
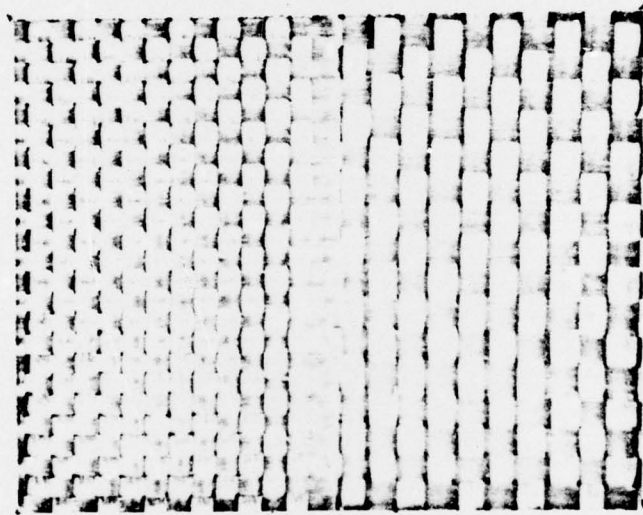


FIGURE 2.
TYPICAL LOAD-DEFLECTION CURVES
FOR 2 INCH WIDE DEN SPECIMENS.



1.0"

FIGURE 3.
WOVEN ROVING FABRIC PRIOR TO
SURFACE TREATMENT.
Left: S-Glass.
Right: E-Glass.

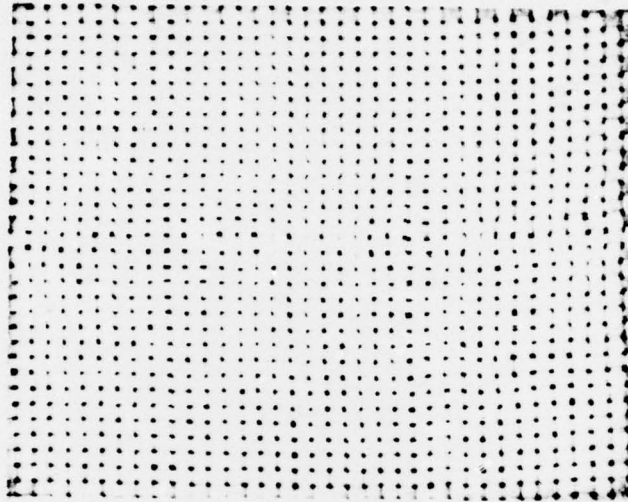


FIGURE 4.
S-GLASS AFTER STARCH-OIL APPLICATION.

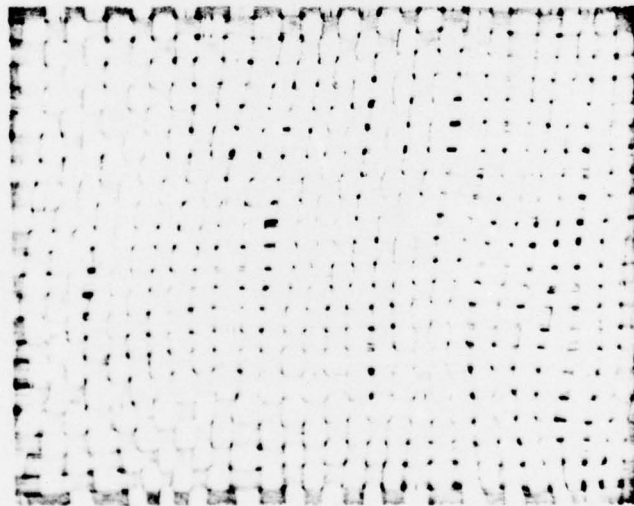


FIGURE 5.
E-GLASS AFTER STARCH-OIL APPLICATION.

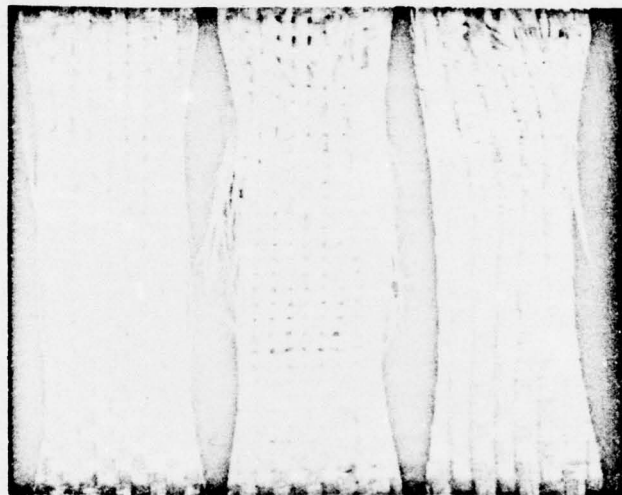


FIGURE 6.
TYPICAL UTS SPECIMENS AFTER FRACTURE.
Left: SC-P (a).
Center: SS-P (a).
Right: ES-P (a).

(a) See Appendix C for key to specimen nomenclature.

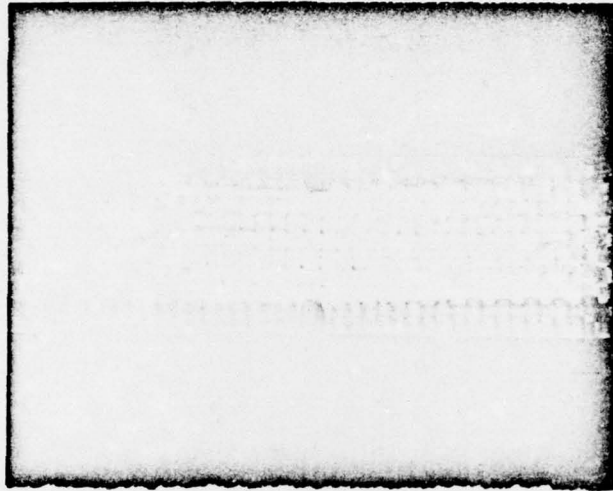


FIGURE 7.
TYPICAL SC-P (a) DEN SPECIMEN.

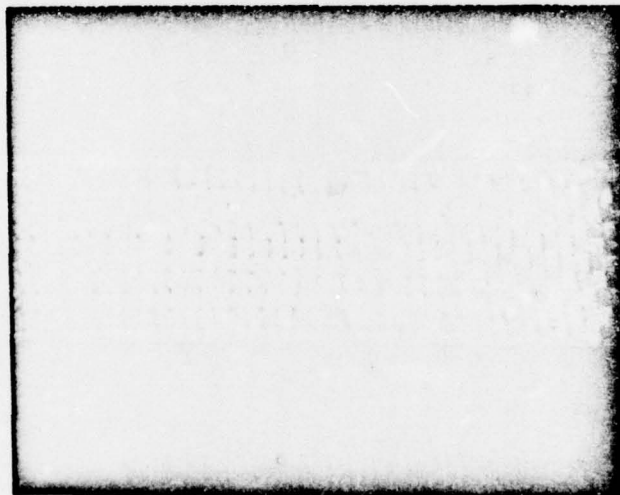


FIGURE 8.
TYPICAL SS-P (a) DEN SPECIMEN.

(a) See Appendix C for key to specimen nomenclature.

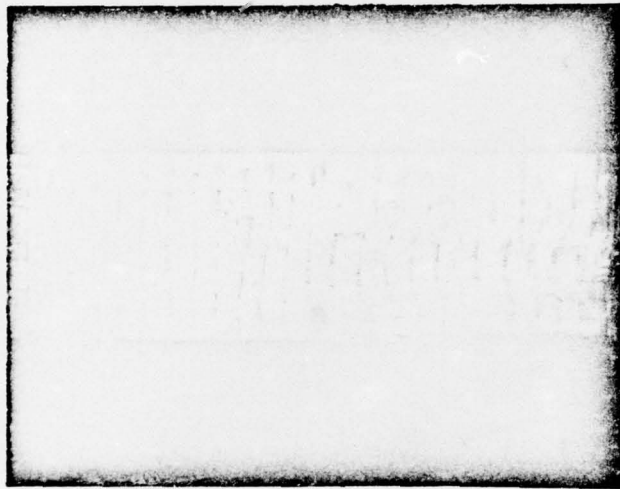


FIGURE 9.
TYPICAL ES-P (a) DEN SPECIMEN.

(a) See Appendix C for key to specimen nomenclature.

